The Influence of Posttetanic Potentiation on Neuromuscular Efficiency in Mouse Fast Twitch Muscle at 25°C

Ryan Laidlaw, BSc. Biomedical Sciences

Applied Health Sciences (Kinesiology)

Submitted in partial fulfillment of the requirements for the degree of

Masters of Science in Applied Health Sciences (Kinesiology)

Faculty of Applied Health Sciences, Brock University
St. Catharines, Ontario

Abstract

Within skeletal muscle the release of calcium is responsible for the initiation of muscle contraction. In addition intracellular Ca^{2+} also induces the protein skeletal muscle myosin light-chain kinase (skMLCK) to phosphorylate the regulatory light chain (RLC) of fast myosin isoforms. For a short time following RLC-phosphorylation a potentiated state is induced within muscle fibres in which force generation and other contraction dynamics are augmented. The intent of our study was to examine the effect of tetanic stimulation (>100Hz) induced potentiation on the efficiency of neuromuscular contraction (Work output: # of Pulses). Concentric contractions were used in which muscles shortened 1.10 -> 0.90 L_o, at ~70% maximal shortening velocity (Vmax). The fast twitch *extensor digitorum longus* muscles were excised and mounted *in vitro* (25^oC) to examine the effect of NME on whole muscle function. Unique to our lab were the use of $skMLCK^{-/-}$ mice which are unable to phosphorylate their myosin-RLC, and thus display no magnitude of posttetanic potentiation. These models were used as a negative control for potentiation compared to the wild type EDL. NME was tested during series of submaximal tetani at five frequencies (10, 25, 40, 55, 80 Hz) before and after muscles were exposed to the conditioning stimulus (4 x 400 msec, 100 Hz, over 10 seconds). Neuromuscular efficiency was found to be increased at all frequencies for both wild type ($P<0.001$) and $skMLCK^{-/-}$ ($P<0.002$) genotypes following the CS (n=12). NME potentiation was significantly impacted by the expression of skMLCK and test frequency. At optimal frequency wild type EDLs displayed a 92% increased relative NME compared to the 33% seen in the $skMLCK^{-/-}$ genotype showing the importance of RLC-phosphorylation to contractile enhancement. Work values preceding the CS

were not significantly different at any frequency in either genotype ($P = 0.236$). The presence of RLC phosphorylation is physiologically significant in enhancing force output as well as improving neuromuscular efficiency following PTP.

Table of Contents:

List of Figures:

List of Tables:

List of Abbreviations:

ADP	Adenosine Disphosphate
ATP	Adenosine Monophosphate
ATPase	Adenosine Triphosphatase
Ca^{2+}	Calcium
CaM	Calcium-Calmodulin Complex
CLP	Catch-Like Property
ECC	Excitation Contraction Coupling
EDL	*Extensor Digitorum Longus*
ELC	Myosin Essential Light Chain
KO	Knock Out
L_o	Muscle Fibre Optimal Length
MHC	Myosin Heavy Chain
MLCP	Myosin Light Chain Kinase
PAP	Post Activation Potentiation
PTD	Post Tetanic Depression
PTP	Post Tetanic Potentiation
RLC	Myosin Regulatory Light Chain
SkMLCK	Skeletal muscle Myosin Light Chain Kinase
TA	*Tibialis Anterior*
TnC	Troponin Calcium binding Subunit
Vmax	Maximum shortening velocity
WT	Wild type

Chapter One: Introduction

Skeletal muscle provides structure to the body and is fundamental for voluntary contraction in mammals. The functional component of skeletal muscle is the motor unit which is comprised of a single α-motor neuron and the group of muscle fibres that it innervates (Milner et al., 1973). Muscle fibres are comprised of many parallel chains of overlapping myosin and actin filaments forming cylindrical structures known as sarcomeres (Craig & Padron, 2004). The myosin protein is a ~554 kDa hexamer whose two head regions each consist of two small protein subunits: the essential light chain (ELC), and the regulatory light chain (RLC), along with two intertwined heavy chains forming the tail region (Craig & Woodhead, 2006; Lowey & Trybus, 2010; Figure 1). The primary interaction between the actin and myosin filaments has been referred to as the cross-bridge cycle and utilizes the hydrolysis of adenosine triphosphate (ATP) to produce contraction (Rayment et al., 1993; Smith, 2018).

The primary influence impacting motor unit function can be attributed to their stimulating motor neuron. Many molecular mechanisms are responsible for impacting motor neuron function including neural modulation (Enoka, 2005). Inputs from the neuromuscular system can have influences on the discharge rate, force generation, and the rate of motor unit recruitment which all contribute to the adaptive responses of skeletal muscle (Heckmann & Enoka, 2012; Enoka & Duchateau, 2017). The impact of neural modulation on whole muscle activity allows for rapid functional augmentation of muscle force during contraction and possibly other unknown effects.

One example of a biochemical modulatory mechanism found in fast skeletal muscle is posttetanic potentiation (PTP) which is defined as the temporally dependent increase in isometric twitch force following previous repetitive activity (Bernhard et al., 1941; MacIntosh et al., 2000; 2008). This mechanism influences muscle activity by causing conformational changes to the myosin-RLC which improves the dynamics of cross bridge formation through increased Ca^{2+} sensitivity (Sweeny et al., 1993). Much remains unknown about the functional significance of PTP in mammalian skeletal muscle. Areas of research include investigation into PTP's role in influencing the dynamics of contraction during fatigue as well as its teleological role (Gittings et al., 2011; Duggal et al., 2014; Bunda et al., 2018). Interestingly, slow twitch muscles appear to display minimal levels of potentiation indicating that it may exclusively be a characteristic of fast skeletal muscle (Hamada et al., 2000). In rats tetanic stimulation (>100 Hz) of slow twitch soleus muscle has been shown to produce a posttetanic depression, rather than potentiation, of isometric twitch force (Buller et al., 1981). Although interactions between fatigue induced force depression and PTP enhancement may confound results, the differences in posttetanic responses may be due to differences in the enzymatic machinery responsible for PTP in fast and slow mammalian skeletal muscle.

Mammalian skeletal muscle possesses one such mechanism leading to PTP, and was elucidated by demonstrating that the magnitude of force potentiation is relative to the extent of myosin RLC-phosphorylation (Vandenboom et al., 1993, 2013). While other pathways may contribute several studies have demonstrated that the activation of the enzymatic machinery responsible for RLC phosphorylation is the primary mechanism leading to PTP (Xeni et al., 2011, Smith et al., 2013, Vandenboom R., 2016). In fast twitch muscle phosphorylation of the myosin

RLC is catalyzed by skeletal muscle myosin light chain kinase (skMLCK) through a calcium directed manner (Kamm & Stull, 2011, Stull et al., 2011). This mechanism appears to enhance force by increasing the calcium sensitivity of the contractile apparatus promoting the sustained formation of cross-bridges (Sweeny et al., 1993, Vandenboom, 2013). A secondary mechanism may involve the direct influence of stimulation induced elevations in resting levels of [Ca^{2+}] (Smith et al., 2013; Vandenboom, 2016).

In the intact neuromuscular system the influence of PTP may extend beyond a simple increase of isometric twitch force. The presence of dynamic afferent feedback pathway(s) could feasibly help regulate skeletal muscle force output under varying conditions. For example the presence of PTP in human skeletal muscle has been shown to depress the action potential discharge rate of motor neurons during submaximal contractions (Inglis et al. 2011; Klein et al. 2001). A reduction in motor neuron activity through potentiation may be advantageous in the conservation of energy and prevention of overstimulation leading to more rapid fatigue onset. Additionally, despite lowered rates of stimulation from the motor neuron units PAP assisted in maintaining consistent augmented force output without recruiting additional motor units to compensate (Klein et al., 2001). The teleological function of PAP in the intact neuromuscular system may be the conservation of energy through increased functional efficiency.

The ratio of muscle force output to the stimulus rate required to elicit said force is referred to as neuromuscular efficiency (Lewis and Barclay, 2014). Based on results from human trials it seems possible that PTP may greatly influence NME in isolated muscle as it does in the intact neuromuscular system. The relationship between PTP and neuromuscular efficiency has not to our knowledge been studied or reported. The purpose of this thesis is thus to examine

the influence of PTP on neuromuscular efficiency using fast twitch muscles from wild type and skMLCK$^{-/-}$ ablated mice.

Chapter Two: Review of Literature

2.1 Skeletal Muscle Structure and Function

I. Motor unit physiology

Motor units are cohorts of muscle fibres grouped into functional segments that are stimulated by a single α-motor neuron. Action potentials discharged by the motor neuron are responsible for the contraction of their innervated fibres. Populations of motor units are activated to transduce muscle contraction into functional movement (Heckman & Enoka, 2012). Motor unit force output is dependent on many factors including both the number fibres controlled by the motor neuron and their respective rates of stimulation. The former is referred to as the motor unit innervation number and can range from hundreds to thousands of fibres for larger muscle groups (Enoka, 1995). The later will be touched on later in this review. Historically motor units have been categorized based on their physiological properties such as fatigue resistance and profile of tetanus. Three distinct types of motor units: fast fatiguing (FF), fast fatigue-resistant (FI), and slow fatigue-resistant (S) were first characterized by Burke et al., (1973) in the muscles of anaesthetized cats. These classifications are useful in research because of the similar, or conserved, stimulation and contractile properties of motor units. However one must consider that all types of motor units function dynamically and that these characteristics are variable based on the composition of the fibres being innervated (Enoka, 2005).

II. Muscle Fibres

As stated, there are many factors impacting the overall functionality of motor units including the composition of muscle fibres. The types of fibres that exist in mammalian skeletal muscle include slow twitch type I fibres as well as fast twitch types IIA & IIB. Skeletal muscle within small mammals also contain fast glycolytic type IIX fibres that possess intermediate fatigue resistance when compared to types IIA & IIB (Schiaffino & Regianni, 2011).The size of muscle fibres can vary from 10 to 100 micrometres in diameter and can be up to several centimeters in length (Craig & Padron, 2004). Type II fibres tend to rapidly contract and heavily rely on glycolytic activity for their function. Type 1 fibres are slower to contract and relax however their reliance on oxidative phosphorylation provides a level of fatigue resistance useful during prolonged contractions (Alnaqeeb & Goldspink, 1987). Variation observed between fibre types is primarily attributed to their respective myosin heavy chain isoform and subsequent adenosine triphosphatase (ATPase) activity (Ennion et al., 1995; Larsson et al., 1991). Differing isoforms of the myosin superfamily illustrate a diverse class of molecular motors suited for certain tasks. In larger mammals myosin heavy chain type II isoform is the most prevalent in skeletal fast twitch muscle (Reggiani et al., 2000). The properties of the myosin heavy chain II isoform are what allow type II fibres to contract more rapidly compared to type I fibres. The caveat is that while fast twitch fibre's enzymatic machinery allows for more rapid function it does so at a lesser efficiency of ATP usage (Shianffino & Reggiani, 2011). The myosin protein from different fibre types are quite conserved; but the specific isoform of MyHC produce different conversion rates of ATP to mechanical energy and are the determinant of overall fibre function (Reggiani et al., 2000, Shiaffino & Reggiani, 2011).

III. Sarcomere Structure

The constituent unit of muscle fibres is the sarcomere which consists of overlapping actin and myosin filaments 1.65 - 3.65 microns in length (Figure 1, Reconditi et al., 2004). In skeletal muscle the primary function of the sarcomere is to generate directional force through its ability to rapidly contract or shorten before relaxation (Craig & Padron, 2004). This is accomplished through the cross-bridge cycle, and characterized by its ability to hydrolyze ATP in a repeatable process (Craig & Woodhead, 2006; Vandenboom, 2016). Actin and myosin together account for a majority of myofibrillar protein, and even as much as 70% of all muscle protein (Actin 20%, Myosin 54%) (Huxley & Hanson 1957; Hanson & Huxley 1957). Proteolytic cleavage of the myosin heads had allowed for structural determination, and discovered highly conserved subdomains of the myosin protein segregated by two loop structures (Loop 1= ATP-binding site, Loop 2= Actin-Binding domain) integral to contraction (Rayment et al., 1993; Vandenboom, 2016). In the relaxed state myosin heads are orderly arranged in a quasi-helical structure with an axial spacing of ~14.5 nm between rows allowing space for head translocation (Wray et al., 1975). Myosin S2 regions form ~150 nm long, ~2 nm thick tails which polymerize into the thick filament backbone allowing for some compliance during the cross-bridge cycle (Chew & Squire, 1995). In all vertebrates the arrangement of the thick filament is conserved and organized into three tracks repeating every ~43 nm (43.5 nm for invertebrates) during the relaxed state (Stewart & Kensler, 1986). In striated muscle, the strict molecular organization of the thick filaments assists in amplifying sarcomeric force generation (Craig & Padron, 2004). Interestingly in smooth and non-muscle cells the repeating array is less organized and more labile, possibly indicating tertiary contractile functions (Craig & Woodhead, 2006).

The other main structural component of the sarcomere is the thin filament actin. Actin is formed from the polymerization of 186 monomer globular actins (G-actin) into long filamentous chains (F-actin) approximately 43 kDa in weight (Koubassova & Tsaturyan, 2011). The actin myosin interaction is the main force producing mechanism, but is assisted by a host of regulatory and accessory proteins that help it in binding to the thick filament such as myosin binding protein C (MyBP-C) (Craig & Padron, 2004). Actin bound proteins such as troponin (Tn) and tropomyosin (Tm) are responsible for the regulation of contraction through Ca^{2+} influx (Koubassova & Tsaturya, 2011). Early work on sarcomere properties showed that the overlap of thick and thin filaments were proportional to the stiffness of the fibre; which demonstrated that the compliance in the acto-myosin complex was variable (Huxley & Simmons, 1973, Ford et al., 1977). Further investigation showed that following tetanic stimulation both actin and myosin relaxed relative to stimulation force. This indicated that partial responsibility for the compliance within sarcomeres came from the filaments themselves (Wakabayashi et al., 1994; Brunello et al., 2014). The remaining elastic property of muscle can be attributed to the actin bound protein titin which is also responsible for enhanced force generation itself through Ca^{2+} activation (Craig & Woodhead, 2006; Powers et al., 2014). Titin is a large protein (3800 kDA) and is sometimes referred to as the third filament due to its integral role in sarcomere relaxation through its elastic properties (Herzog et al., 2015).

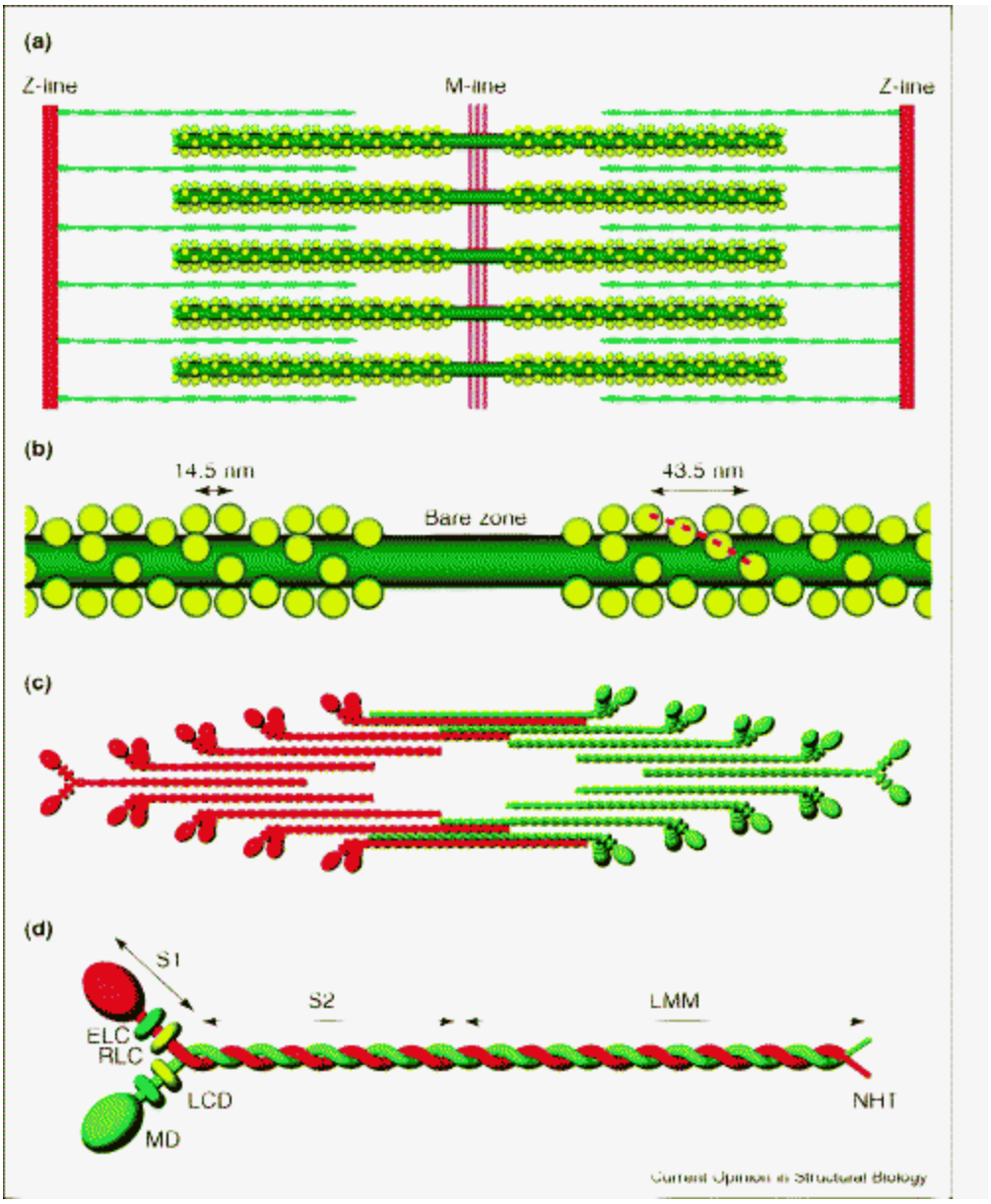

Figure 1: Structural arrangements of myosin and the sarcomere. (Craig & Woodhead, 2006)

(A) Striated muscle sarcomere. (B) Myosin Center Portion - Helical Array Arrangement. (C) Overhead view of thick filament orientation. (D) Myosin Molecule. Head regions (S1) each consisting of ELC and RLC subunits; and intertwined heavy chain tail region (S2).

IV. The Cross-Bridge Cycle

Neuromuscular signals are transduced into functional movement through the cross-bridge cycle which is an ATP requiring process. This was first investigated by HE Huxley & Hanson (1954), and later summarized by AF Huxley & Neidegerke (1954), introducing the first conception of the sliding filament theory. Through different experimental methods these two groups came to the conclusion that sarcomeres shorten through the sliding of actin and myosin filaments which is the foundation of our current understanding.

The cross bridge cycle begins in the inactivated state before the discharged action potential causes the release of Ca^{2+} from the sarcoplasmic reticulum. Until this occurs the regulatory proteins Tn and Tm reside on the thin filament and sterically block binding sites preventing the formation of the acto-myosin complex (Gordon et al., 2000). Troponin is comprised of three subunits with varying functions; TnC functions as a Ca^{2+} sensor possessing greater number of Ca^{2+} binding sites in fast (2 high 2 low Ca^{2+} affinity) muscle compared to slow muscle (2 high 1 low) (McKilop & Geeves, 1993). The TnT subunit appears to be the structural 'glue' that holds the troponin complex together as it binds to actin, TnC, and Tm; while TnI is responsible for linking intra-molecular movements (Perry, 1998). Tropomyosin is an elongated molecule ~42 nm long and formed from the homo- or hetero-dimerization of two alpha helical chains (Gordon et al., 2000). Tm normally resides dormant and bound to actin until a 25 degree translocation of the COOH- terminal end is caused by Ca^{2+} binding to Tn (Phillips et al., 1986; Lehman et al., 2001).

The force generation process begins when ATP hydrolysis occurs in the nucleotide binding pocket of the myosin head causing conformational changes (Gordon et al., 2000). Once

the Ca^{2+} influx causes Tm and Tn to be translocated away on the thin filament, one myosin head binds actin forming the acto-myosin complex (Gordon et al., 2000). The power stroke is initiated with the release of a phosphate molecule while the myosin heads pulls the thin filament towards the midline of the sarcomere. It is the movement of the S1 portion of myosin that is responsible for sarcomere shortening; however the ATPase rate is dependent upon the specific isoform of the myosin motor (Sheetz & Spudich, 1983; Rayment, 1996). After the power stroke is complete an ADP molecule is released from the S1 binding pocket providing room to attract another ATP molecule. The acto-myosin complex detaches after the myosin head binds to a new ATP and returns to the non-force generating state (Gordon et al., 2000). When myosin cross bridges are bound to actin they are able to rapidly detach and cycle allowing for the sliding of filaments which reduces the time it takes for muscle force redeployment (Vandenboom et al., 2002). Myosin cross bridges are also able to delay detachment from actin following the Ca^{2+} transient which extends the time spent in the force generating state (Patel et al., 1998).

V. Regulation of Contraction

The basis for voluntary contraction in skeletal muscle is based on the thick filament, but is primarily regulated by the thin filament. The primary method of regulation comes from the steric hindrance of Tn and Tm blocking the myosin binding sites on actin (Gordon et al., 2000). The thin filament binding sites remain inactive until the TnC subunit binds to Ca^{2+} with high affinity, which then promotes the translocation of the blocking proteins (Gordon et al., 2000). This is important because the rate of early force development depends mostly on the extent of Ca^{2+} mediated activation of the thin filament (Silva & Reinach, 1991). This regulatory

mechanism has been summarized by McKillop and Geeves, (1993) into a three-state model in which myosin binding sites on the thin filament can either be open, closed, or blocked relative to their level of activation (Figure 2). Once Tm and Tn have been shifted away, the 'closed' binding site is free to form weak cross bridges with myosin heads. Ca^{2+} activation along with partial cross bridge formation produces conformational changes that cause the myosin binding site to shift to an 'open' state, and promoting the formation of additional actomyosin complexes (Moraczewska, 2002). This is one pathway in which cooperative activation by the thin filaments exacerbates cross bridge formation.

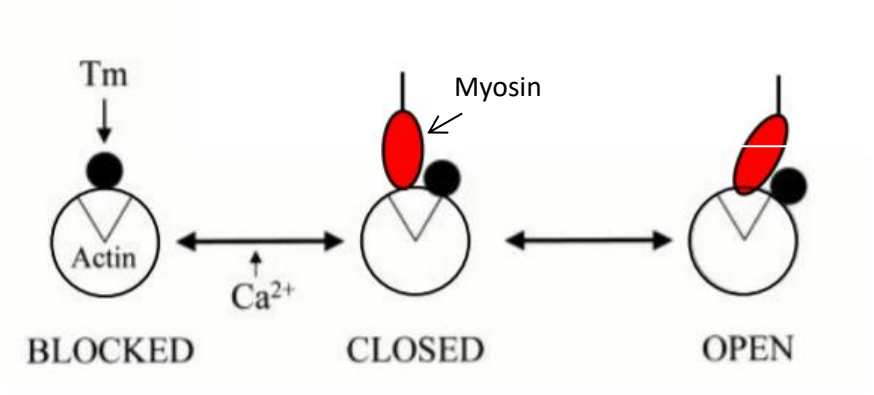

Figure 2: Three state model of thin filament activation. The initial state of actin is the 'blocked' state in which tropomyosin sterically blocks myosin binding sites. Upon Ca^{2+} activation Tm is translocated away allowing for myosin-actin binding before proceeding to the active 'open' state. (McKilop & Geeves, 1993)

Due to the flexibility of Tm, myosin affinity for actin is variable along its surface which has led to the establishment of a thin filament regulatory unit. This established unit contains 7 actins: 1 tropomyosin: 1 troponin ($A_7T_mT_n$) (Gordon et al., 2000). Strong actomyosin bindings within an actin regulatory unit are known to promote Tm movement in neighbouring $A_7T_mT_n$ units as well, promoting additional cross bridge formation (Gordon et al., 2000). This mechanism shows how actin structurally maintains the 'open' status of the myosin binding sites

and is another example of how the thin filament promotes cooperative activation leading to contraction.

The thick filament also possesses mechanisms responsible for the regulation of the cross bridge cycle. X-ray evidence has shown populations of myosin heads folded towards the center of the sarcomere, seemingly inactivated, which could not bind to actin nor hydrolyze ATP (Woodhead et al., 2005; Stewart et al., 2010). High force generation requires a majority of myosin heads to form cross bridges during contraction, which lead to inquiries into how inactivated myosin senses the thin filament during contraction (Piazzesi et al., 2018). The property of mechanosensing was proposed by Linari et al., (2015), elucidating the mechanisms by which inactive myosin heads are recruited relative to filament stress. The activation of thick filaments is accompanied by an increase in the movement range of myosin S1 that better aligns the interacting head motif for cross bridge formation compared to the inactive state (Alamo et al., 2008). Thick filament's ability to regulate the amount of available myosin heads available for binding, and actin's means to monitor available myosin binding sites though Tn and Tm, make up the dual filament theory of skeletal muscle regulation (Piazzesi et al., 2018).

VI. Motor unit recruitment patterns

In voluntary contractions the sequence of motor unit recruitment is generally ordered and follows size dependency based on their associated α-motor neuron diameter. Described by Henneman (1957), the size principle states that smaller motor neurons are activated prior larger motor neurons. Smaller motor units possess smaller diameter neurons which generally innervate slow twitch fatigue resistant muscle fibres. In contrast larger motor neuron somas

typically innervate greater numbers of fast twitch fibres. This property describes the relationship between motor neuron soma size and recruitment order illustrating the normal functionality of muscle fibres. The benefit of recruiting smaller motor units first is the conservation of fatigue in larger muscle fibres as well as only activating fatigable fast twitch fibres when high force is required. However the characterization of motor units using the size principle is problematic because neurons commonly innervate a composition of fibre types (Enoka, 2005). Therefore while ordered recruitment of motor units generally progresses from smallest to largest due to conduction speeds of motor units; it does not necessarily mean slow twitch muscle types get recruited before fast twitch muscles.

Size dependency is a characteristic of motor neurons observed throughout all muscles in the body however the functional advantages are contentious (Milner-Brown, *et al.,* 1973; Stein *et al*., 2005; Dideriksen & Farina, 2013). In terms of optimal muscle performance it was found that size-ordered recruitment of motor units did not out preform random recruitment patterns and that the primary influence of force production was innervation number. A range of motor neuron soma sizes exist and their respective thresholds are linked to the number of fibres that they innervate. This implies that universally-observed ordered recruitment of motor units may not be a method to providing functional optimization and instead accounts for the range of excitabilities among various sized motor units (Dideriksen & Farina, 2013). Muscle fibre type is also in part determined by the stimulation produced from the motor neuron (Sargeant, 2007). It is well characterized that muscle fatigue causes a decline in muscle force output following previous activity. Work by the De Luca group demonstrated that under the effect of fatigue the recruitment threshold for motor neurons universally becomes lowered; yet ordered

recruitment remains conserved (Adam & De Luca, 2003). At high levels of voluntary contraction force it is observed that the number of motor units available for recruitment declines yet force is still able to increase (Milner-Brown, *et al.,* 1973). Since the recruitment pattern for motor units remains unchanged during fatigue then other factors must be modulated to compensate for the loss of force output.

2.2 Motor Unit Firing Rate

Another major constituent of voluntary contraction force is motor neuron discharge rate (rate coding). The frequency of action potentials discharged from the motor neuron is the primary factor of force production except in low force contractions (Enoka & Duchateau, 2017). The effect of rate coding on muscle force can be classically observed from the force-frequency relationship in which stimulation frequency and muscle force output are relative to one another, but declines during high levels of force generation (Macefield et al., 1996). Variation in single fibre force output can vary by 3-15x relative to changes in stimulation frequency (Enoka, 1995). Since many thousands of individual motor units must be activated for functional movement they must each produce levels of force appropriate to the demand. Progressive increase of muscle force generation requires both recruitment of additional motor units and higher rates of stimulation (Enoka & Duchateau, 2017). The disparity in force production between types of motor unit types is primarily due to the variation of stimulation frequency (Enoka, 2005). Control of motor neuron discharge frequency is responsible for the dynamic

modulation of force and indicates a scheme for the regulation of muscle force development (De Luca & Erim, 1994).

I. Rate Coding Regulation

The mechanisms that regulate rate coding have been investigated for many decades. The discharge rate of motor neurons is dictated by the synaptic input that it receives from the CNS (Enoka & Duchateau, 2017). Rate coding is influenced by the inward currents produced by changing neuro-modulatory inputs to the motor neuron pool (Heckman & Enoka, 2012). In addition motor neuron activity is heavily modulated by inputs through ligand-gated ion channels. Common ionic inputs can alter discharge frequency of motor neurons and describes a CNS derived regulatory mechanism of rate coding (Binder et al., 2010). These signals are produced from ligand-gated channels and are able to evoke excitatory and inhibitory postsynaptic potentials. Neurotransmitters that influence rate coding include serotonin and norepinephrine (Enoka & Duchateau, 2017). Serotonin binding to its receptors (5-HT) has an excitatory effect on motor neuron discharge rate and results in increased force output over the duration of contraction (Perrier & Cotel, 2015).

Over prolonged voluntary contractions muscle fatigue sets in and results in the failure to maintain force. To maintain muscle force output throughout prolonged contractions, the decline in force from fatigue must be supplemented. This is achieved primarily through increasing the stimulation rate of motor neurons (Enoka & Duchateau, 2017). Since the fundamentals of size based recruitment of motor units are invariant through fatigue the CNS is

responsible for adjusting the threshold of stimulation sensitivity to the motor neuron pool (De Luca et al., 2014). A majority of investigations use isometric contractions to observe the firing behaviour of motor neurons. However exceptions to the normal firing pattern were observed in high frequency oscillatory contractions. The De Luca et al. (2014), group also observed that during oscillatory contractions the stimulation frequency of lower threshold motor units effectively decreases while higher threshold motor unit stimulation increases. This transposition of firing rates demonstrates a preferential activation of high threshold motor units which is an exception to the hierarchical regulation scheme (De Luca et al., 2014).

Utilizing anaesthetized cat muscle it was initially hypothesized by Eccles et al., (1958) that large higher threshold motor neurons exhibited a higher stimulation frequency compared to lower threshold units. They had hypothesized that the duration of after-hyperpolarization played a significant role in regulation and concluded that earlier recruited motor neurons generally have a lower firing rate compared with later recruited motor units (Eccles et al., 1958). They assumed this on the basis that voluntary contractions would produce an ideal fused tetanus optimized for prolonged contractions. However this hypothesis was inaccurate. Instead much research has been done to display the opposite phenomena of rate coding; that higher-threshold motor units have lower firing rates compared to lower earlier-recruited motor units (De Luca & Hostage, 2010; Holobar et al., 2009). The inverse relationship between rate coding and recruitment threshold at any level of force has been termed the ‘onion skin’ motor unit control scheme, and appears to be conserved throughout contraction (De Luca & Contessa, 2015). This regulation method allows for effective economy of force generation in lower

threshold motor units and reduces the effects of fatigue in later recruited units (De Luca & Contessa, 2012).

II. Catch – Like Property

The catch-like property is a phenomenon of skeletal muscle that can augment the summation and subsequent maintenance of force (Burke et al., 1970). CLP is initiated after two or more closely spaced action potentials stimulate a motor unit, but it remains unclear whether this represents normal discharge patterns or are spontaneous 'errors' of neuromuscular transmission (Garland & Griffin, 1999, Gittings et al., 2016). As opposed to PTP the magnitude of CLP influence appears to be greater in slow twitch muscle rather than fast due to increased sensitivity to bouts of high frequency stimulation (Burke et al., 1970). The molecular pathway(s) leading to CLP induction are not fully understood however it does not appear to be caused by changes in neuromuscular transmission nor to motor neuron excitability (Burke et al., 1976). A proposed mechanism is that the high force levels generated from two closely space stimulations rapidly stretch the series elastic component of the sarcomere increasing muscle stiffness and may work to amplify mechanical force transmission between sarcomeres (Binder & Barrish, 1992, Nielson, 2009, Gittings 2016). Alternative mechanisms that modulate skeletal muscle force production such as potentiation are significantly important in interactions with CLP, and maintaining muscle force throughout fatigue (Ding et al., 2003).

2.3 Skeletal Muscle Force Potentiation

Potentiation is a property exclusive to fast twitch muscle in which isometric twitch force increases following previous activity (Vandenboom, 2016). Previous studies have shown that the magnitude of RLC phosphorylation and resulting twitch force potentiation are relative to one another indicating (Vandenboom et al., 1997; Xeni et al., 2011). Widespread presence of potentiation amongst skeletal muscle indicates that it is a normal feature of fast twitch fibre function (Brown & Loeb, 1998). Potentiation is manifested in two forms depending on a myriad of factors the primary being frequency of stimulation. During low frequency stimulation of skeletal muscle staircase potentiation is induced in which there is a step-wise progressive increase in isometric twitch force compared to the unpotentiated muscle. However high frequency stimulation of fast skeletal muscle induces posttetanic potentiation (PTP) leading to sustained increases of work and power output through increased Ca^{2+} sensitivity (Vandenboom et al., 2013). In a physiological setting it has been proposed that the potentiated state of skeletal muscle is the normal operating level opposed to unpotentiated muscle (Brown & Loeb, 1998). When RLC phosphorylation is absent due to skMLCK ablation PTP is completely lacking from fast twitch muscle fibres. However the amount of staircase potentiation is only attenuated by up to 50% (Gittings et al., 2011; Zhi et al., 2005). This indicates that there may be complementary physiological mechanisms responsible for the induction of potentiation. Indeed, work by the Smith et al., (2013) group investigated the role of intracellular calcium levels and handling in mouse lumbrical muscles. They concluded that stimulation induced [Ca^{2+}] elevations produced a small magnitude, short lived potentiation of isometric twitch force (Smith et al., 2013). Since the time span for this form of potentiation is so brief functional

utilization is unachievable in a physiological setting. Therefore the effect of lasting twitch force potentiation can be primarily attributed to the RLC-phosphorylation induced pathway.

I. Myosin RLC Phosphorylation

As stated the head of the myosin thick filament contains two small protein subunits; the regulatory light chain (RLC) and the essential light chain (ELC). These subunits wrap around the alpha-helical neck region of the heavy chain providing structural support (Lowey & Trybus, 2010). Moreover myosin II RLC contains a binding domain region that is easily phosphorylated. This is accomplished through the Ca^{2+}/calmodulin dependent enzyme skeletal muscle myosin light chain kinase (skMLCK). The phosphorylation event is known to alter the structure function relationship of myosin S1 relative to the thick filament through translocation of the myosin head (Vandenboom, 2016). Indeed, work by Levine et al., (1995, 1996), showed RLC phosphorylation introduced a 2.5 - 5.5 nm increase in spacing distance between individual myosin heads. The translocation myosin heads allow the formation of the actin-myosin complex at a higher affinity compared to pre-phosphorylation (Sweeny et al., 1993; Colson et al., 2010). Phosphorylation of the RLC is closely associated with the enhancement of contractile performance and generates the temporal dependent state potentiation in fast twitch muscle (Stull et al., 2011; Vandenboom et al., 2013).

II. Regulation of RLC Phosphorylation

Since the control of muscle force output can be modulation by RLC-phosphorylation induced potentiation it must be tightly regulated. The specific kinase responsible for the RLC-phosphorlyation event in fast skeletal muscle is myosin light chain kinase (skMLCK). Interestingly, this protein's function is well described in fast muscle, but is completely absent from slow twitch skeletal muscle (Vandenboom, 2016). The activity of skMLCK has shown to be dependent on the secondary messenger Ca^{2+}- activated calmodulin (Stull et al., 2011). SkMLCK contains a Ca^{2+} dependent auto-inhibitory sequence located between the catalytic core and calmodulin binding motifs that normally holds skMLCK in an inactive state, and prevents its kinase activity (Padre & Stull, 2000; Stull et al., 2011). Ca^{2+} release from the sarcoplasmic reticulum precedes thin filament activation through troponinC, and also saturates the protein calmodulin forming the Ca^{2+}/calmodulin complex. This complex then undergoes conformational changes that increase the affinity for binding with skMLCK resulting in enzyme activation (Stull et al., 2011). Bound/activated skMLCK displays an exposed catalytic site that allows the N-terminus of RLC to enter. The negatively charged phosphate provided by an adenosine triphosphate (ATP) is then transferred to a serine-threonine residue of the regulatory light chain while ADP is released (Stull et al., 2011).

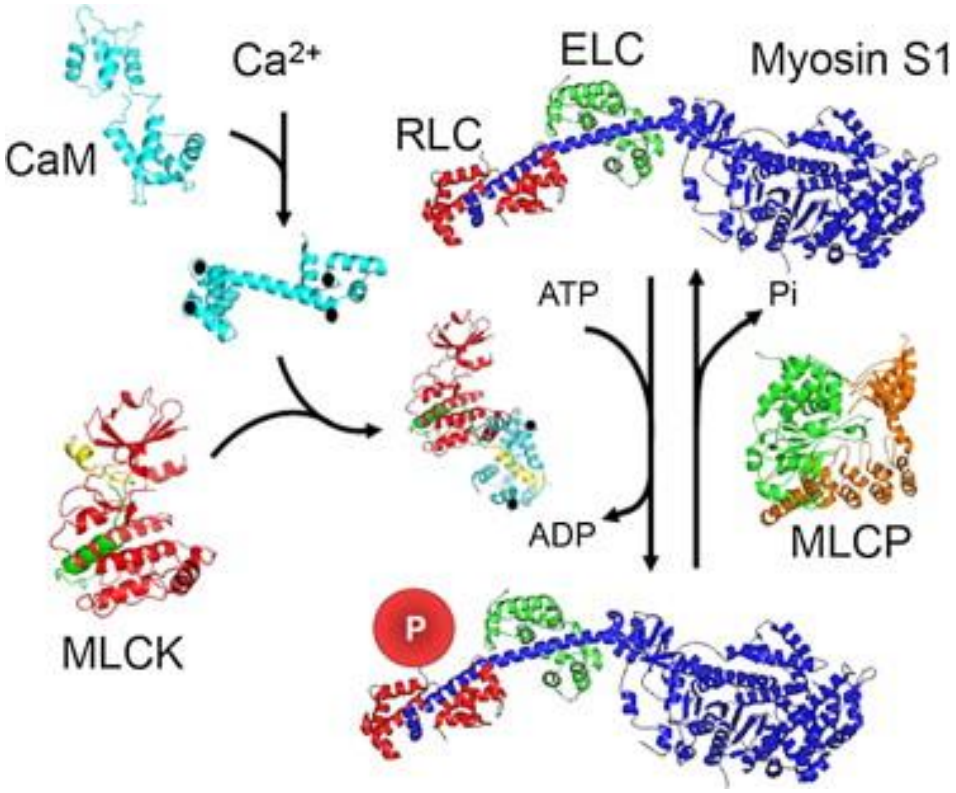

Figure 3: Regulation of myosin RLC phosphorylation in skeletal muscle. Influx of Ca^{2+} from the sarcoplasmic reticulum binds calmodulin (CaM) forming the Ca^{2+}/Calmodulin complex which in turn activates skMLCK. Activated skMLCK utilizes a hydrolyzed ATP to phosphorylate serine residues present on myosin RLC leading to PTP. The reverse process is regulated by myosin light chain phosphatase (MLCP) which removes the phosphate from myosin RLC and operates at a static rate (Stull et al., 2011).

Association of the Ca^{2+}/calmodulin complex with skMLCK occurs with high affinity as shown by its low rate of dissociation (0.03 s^{-1}). The process is also very rapid to form rapid (10^{-7} M^{-1} S^{-1}) and slow to disassociate prolonging the duration in which muscle force output it potentiation (Gallagher et al., 1997). In contrast, the antagonistic enzyme responsible for the de-phosphorylation of myosin RLC is myosin light chain phosphatase (MLCP) (Morgan et al., 1976; Hartshorne et al., 2004). Notably the activity of MLCP is not dependent on the Ca^{2+}/calmodulin complex instead remaining functional at resting levels of Ca^{2+} and operates at a

static rate compared with skMLCK (Manning & Stull, 1982). Therefore due to differing catalytic rates the state of phosphorylated RLC exists for an extended duration before the rate of MLCP can catch up. The downstream effect of this is a prolonged state of PTP in fast muscle fibres and hence has been referred to as the molecular memory of contraction (Stull et al., 2011; Vandenboom et al., 2013). Interestingly, Decostre et al., (2000) reported that beta-adrenergic stimulation through adrenaline prolongs the state of potentiation from RLC phosphorylation in fast twitch muscle. They hypothesized that the presence of adrenaline could inhibit the activity of MLCP indicating a tertiary mechanism to exacerbate the effects of potentiation. Beta-adrenergic stimulation may act in synergy with RLC phosphorylation induced potentiation during rapid fight of flight scenarios (Decostre et al., 2000).

III. Post Tetanic Depression

Secondary mechanisms of RLC phosphorylation regulation include relative expressions of the kinase skMLCK and the phosphatase MLCP (Vandenboom, 2016). The primary factor of RLC phosphorylation extent is skMLCK activity which is most prominent in fast type (IIx & IIb) fibres and least prevalent in slow type (I and IIa) fibres (Smith et al., 2013). This is why potentiation generally requires very high stimulation frequency in slow skeletal muscle, and even then is attenuated as well as slower to occur (Vandenboom, 2016). Instead, a posttetanic depression was demonstrated following tetanic stimulation (100 Hz for 300 ms) in cat soleus (slow) muscle (Buller et al., 1981). Depression of isometric twitch tension at varying tetanic frequencies (50, 100, and 200 Hz) was observed and ultimately accelerated the relaxation phase of the twitch (Buller et al., 1981; Close and Hoh, 1969). Interestingly the same thing can be seen

in *fast* skeletal muscle during *unfused* tetani and also when a high stimulation frequency bout immediately follows a lower one (Celichowski, 2005; Celichowski et al., 2011). Since posttetanic depression is observed in both muscle phenotypes after only the *initial* pulse interval, it can effectively influence force regulation during voluntary contraction (Celichowski et al., 2011).

IV. Potentiation Mediated Muscle Function

Potentiation through myosin phosphorylation characteristically enhances the force and work output of mammalian fast twitch skeletal muscle. This can be translated to improved physiological function at the level of the motor unit. It is established that skMLCK mediated RLC phosphorylation increases the sensitivity of the motor unit to [Ca^{2+}] during contraction in permeabilized fibres (Vandenboom et al., 2013). Following tetanic stimulation RLC phosphate content is observed to dramatically increase up to nine-fold while the peak rate of force development also rises (mean 27%) (Vandenboom et al., 1993). However differences in peak isometric twitch force were discovered between rates of stimulation compared to non-potentiated muscles. Lower stimulation rates (1-15Hz) of potentiated mouse EDL were found to produce the greatest increase of isometric twitch force (~15%) while higher stimulation rates (20-150Hz) depressed peak force (5-40%) feasibly due to fatigue (Vandenboom et al., 1993). Due to the short time period following contraction it is unlikely that the magnitude of [Ca^{2+}] release or levels of buffering were altered (Smith et al., 2013). Increased speed of force development may be due to the motor unit's lower requirement of [Ca^{2+}] for activation post-

potentiation resulting in more units being readily recruited and higher rates of stimulation. Effect the conditioning stimulus on concentric force traces can be seen in figure 9.

V. Potentiation- CLP Interaction

In skeletal muscle, the presence of both posttetanic potentiation and the catch-like property demonstrate redundant mechanisms to modulate contractile function leading to increased force output. Despite the apparent redundancy, their coexistence may indicate evidence that each has functional utility whether operating independently or not. Indeed, work by Gittings et al., (2016) demonstrated an interaction in which the magnitude of the CLP was diminished after induction of PTP in the fast muscle phenotype (Figure 4). This is thought to be caused by RLC phosphorylation mediated enhanced Ca^{2+} sensitivity limiting the effectiveness of increased Ca^{2+} thin filament activation from the initial pulses and negatively impacting the CLP (Ding et al., 2003; Gittings et al., 2016). These results showed that while PTP is more prominent in the fast muscle phenotype, both mechanisms have physiological utility in muscle function.

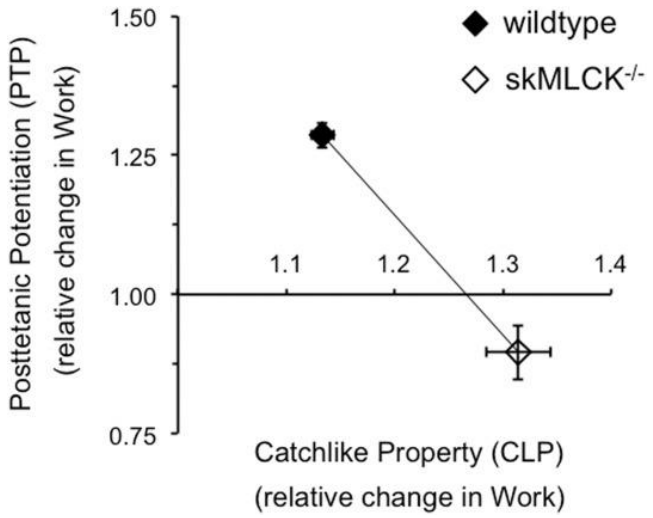

Figure 4: Association of posttetanic potentiation (PTP) and the catch-like property (CLP) in wild-type and skMLCK-/- muscles. PTP values were calculated as the average degree of potentiation of muscle work. CLP values were calculated as the mean work enhancement in both potentiated and unpotentiated muscle. The graph shows the relationship between two force enhancement mechanisms when PTP is present (WT) and absent (skMLCK-/-) illustrating a negative interaction (Gittings et al., 2016)

2.4 Contractile economy

The effect of potentiation has also been examined in terms of contractile economy representing the mechanical output in relation to metabolic input. A lower rate of high energy phosphate usage from ATP would be physiologically significant in improving the efficiency of motor unit contraction and conservation of energy. Gittings et al., (2018) had demonstrated that following high frequency generated potentiation (PTP) there were no statistical differences in phosphate usage between WT and skMLCK$^{-/-}$ mice (19.03 +- 3.37 and 16.02 +- 3.41 µmol respectively) despite the increased amount of force produced by the WT cohort. Their result concludes that RLC phosphorylation enhances dynamic contractile function in mice, but does so without decreasing the efficiency of contractile economy. During low frequency induced

staircase potentiation this result was confirmed though the elevation is RLC phosphorylation in WT mice compared to skMLCK-/- (~3.5x greater) caused statistical differences in high energy phosphate consumption (Bunda et al., 2018).

I. Neuromuscular Efficiency

Finally, rate coding is another aspect of motor unit function that is influenced by the induction of potentiation. An improved amount of force generated per individual stimuli would be advantageous in maximizing muscle fibre output. This interaction was investigated in human triceps brachii by Klein et al., (2001) who demonstrated that during brief voluntary contractions motor unit discharge rate declined significantly (1-6Hz) following the induction of potentiation compared to un-potentiated muscles. The decrease in discharge rate was significantly correlated with the increase of potentiated twitch force (r=-0.74) while no evidence of additional motor unit recruitment was found. In contrast, no decline in rate coding and little association with potentiated twitch force (r=0.06) was found in the same muscle group in elderly males after conditioning (Klein et al., 2002). This suggests an age-related modification in the neural scheme for adjusting motor unit output. Another study examined prolonged contractions illustrating that discharge rates do initially decline, but the maintenance of voluntary force may be supplemented through the potentiation (De Luca et al., 1996).

Further evidence of improved neuromuscular efficiency via potentiation is presented by Inglis et al., (2011) in the lower extremity human *tibialis anterior* muscle. After establishment of PAP, the rate of neuron discharge was significantly depressed from 20.3+- 0.8 (before) to 18.3+- 0.99 (after) pulses/s^{-1} (~10%) as well as reduction in mean power frequency by ~9%.

They indicate the presence of an afferent feedback pathway that depresses rate coding when motor units are enhanced by PAP which may compensate for neuromuscular fatigue. However during prolonged fatiguing contractions discharge rates initially decline before later increasing with the recruitment of additional motor units to maintain force (Adam & De Luca, 2005). This phenomenon appears to incorporate the functional aspects of potentiation while maintaining the inverse relationship between firing rate and recruitment threshold during fatiguing contractions.

Chapter Three: Statement of the Problem

Investigation into fast muscle RLC phosphorylation-mediated force potentiation has revealed much about its modulatory aspects during normal muscle function (Vandenboom, 2013). RLC phosphorylation induced modification to skeletal muscle function has primarily been characterized as the increase in isometric twitch force following previous tetanic stimulation (Vandenboom, 2016). However other mechanisms by which PTP can influence dynamics of muscle contraction have been explored. For example, in human *tibialis anterior* muscle the induction of potentiation depressed neuromuscular discharge rates during submaximal contractions whilst generating a 260 +- 16% increase in maximum voluntary contraction (MVC) force (Inglis et al., 2011). Studies by Klein et al., (2001), have shown similar results in human *triceps brachii* demonstrating a significant decline (1-6Hz) in motor unit discharge rate following establishment of PTP through tetanic contractions. Clearly potentiation has the potential to

influence motor neuron stimulation rate but possibly other dynamics of contraction to modulate muscle force output.

A remaining question regarding the influence of RLC phosphorylation induced changes to muscle function concerns the influence of PTP on neuromuscular efficiency (*i.e.* the ratio between stimulation rate and muscle force). Mammalian fast twitch muscle's ability to increase force via skMLCK mediated phosphorylation of the myosin RLC may have other influences on the dynamic control of potentiated motor units. Although evidence of this relationship has been obtained in the intact human neuromuscular system it remains to be determined if this outcome was due to the RLC phosphorylation or to other unidentified mechanisms (Adams et al., 2005; Inglis et al., 2011).

3.1 Purpose & Hypotheses

The purpose of this study was to investigate the effect of PTP on neuromuscular efficiency (Total Concentric work: # of pulses) in fast twitch skeletal muscle. This effect was studied in vitro (25°C) within fast skeletal muscle (EDL) from wild type (WT) and skMLCK $^{-/-}$ mice.

I. Expected result: Posttetanic potentiation increases Neuromuscular Efficiency

We hypothesized that the induction of PTP will significantly improve neuromuscular efficiency (Total Concentric work/ # of pulses) compared to before the conditioning stimulus. Alternatively, since skMLCK$^{-/-}$ muscles display a residual level of PTP, one expects that this genotype will display a smaller change in neuromuscular efficiency compared to WT muscle.

Chapter Four: Methodology

I. Mice Models and Housing

This study was approved by the Animal Care Committee of Brock University: AUP# 20–04–01

The wild type (WT) mice (22.2 ± 1.72g, 8-12 weeks) used in this experiment were purchased from Charles River Laboratories (C57BL/6) and were transported to Brock University for housing. The skMLCK$^{-/-}$ KO mice (23.1 ± 2.04g, 8-12 weeks) were selected from our breeding colony kept on site. All test animals were kept within the Comparative Bioscience Facility (CBF) at Brock University according to CCAC guidelines and following SOPs:

- HUSB04 - Care and maintenance of mice
- EE02 – Environmental enrichment for mice

Animals Allotted for Study:

- 20 WT C57BL/6 Mice (10 Male & 10 Female)
- 20 skMLCK KO Mice (10 Male & 10 Female)

II. Surgical Protocol

All procedures were carried out in Brock's center for bone and muscle health (CRN434). Prior to experimentation mice of either genotype were selected and transported to our lab from the CBF in a covered container (SOP #SAFE06 – Transportation of Laboratory Rodents within the University). Mice were then fully anaesthetized via the inhalation of isoflurane gas (SOP #HEAL25 – Use of isoflurane in rodent surgeries using a vaporizer). Two *extensor digitorum longus* (EDL) were surgically excised from the hind limbs of each mouse under full anaesthesia (Figure 5). Euthanasia was then administered via cervical dislocation (SOP #-

EUTH04 – Methods of euthanasia for various animals) and the remains stored in the freezer (CRN177) until disposal occurred.

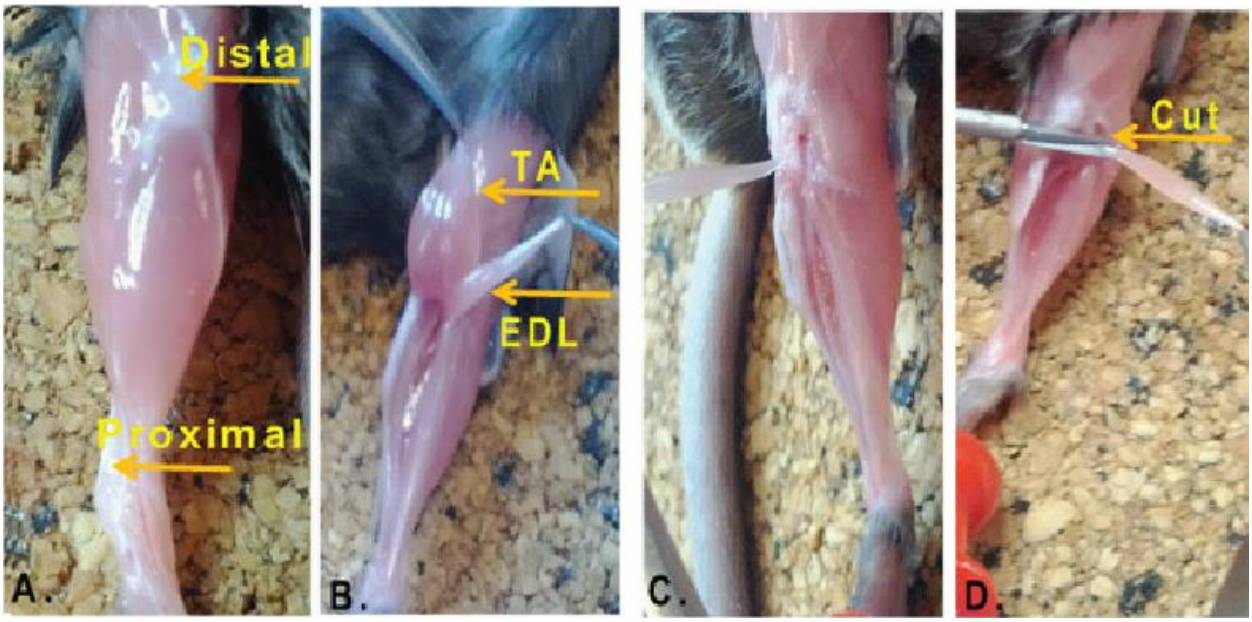

Figure 5: Rodent hind limb musculature and EDL excision. The *extensor digitorum longus* muscle lies underneath the *tibialis anterior.* Muscles were securely sutured at the proximal and distal tendons before attachment to the length-force transducer.

III. Preliminary Experimental Protocol

Rapidly after excision, the EDL muscles were mounted to a vertical organ bath system (Model 305B Aurora Scientific Inc.). Both proximal and distal ends of each muscle were first securely sutured with suture and attached to either the servomotor/force transducer end or anchor point (Figure 6). While attached to the equipment the muscles were immersed in Tyrode's solution (Lannergren et al., 2005) and continuously perfused with oxygen (95% O_2, 5% CO_2) to sustain specimen integrity. Stimuli were administered via flanking platinum wire electrodes utilizing the function of the Model 701B stimulator (Aurora Scientific Inc.)

EDL muscles were initially stretched to ~3-5 mN of resting tension and allowed rest before being stimulated with a brief (300ms) high frequency (100 Hz) stimulus to remove any compliance from the secured muscle. Muscles were then subject to a one hour equilibration period during which they were briefly stimulated with twitches every three minutes. Afterwards, optimal length for force generation was experimentally determined through a series of test contractions (± 0.5 mN resting tension). Muscle length was recorded manually using vernier calipers and set as L_O for the following steps. At the same time the other excised muscle was contained in a holding bath while the first experiment occurred. N = 12 muscles were used from each genotype. All muscles used in this experiment were subjected to the same protocol. Length and force data collection was accomplished via *Linus* Linux software.

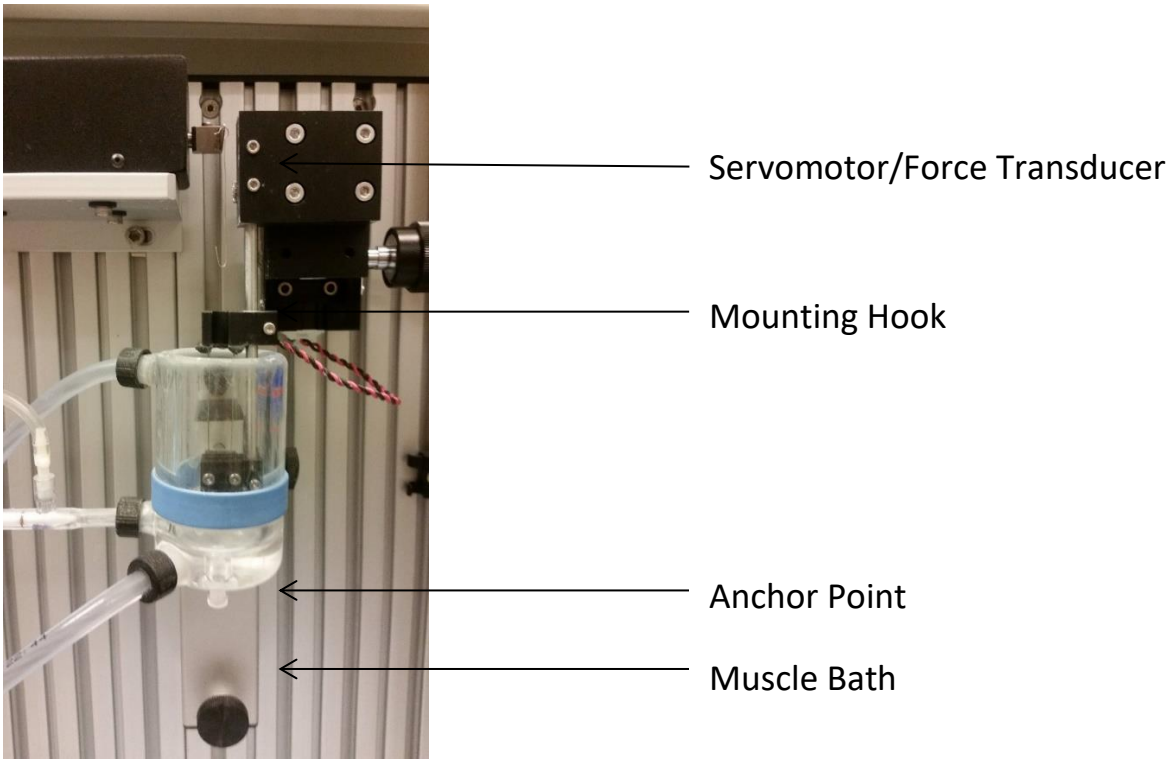

Figure 6. Vertical Muscle Organ Bath System (Model 305B, Aurora Scientific Inc.) Muscles were securely fastened to the apparatus with surgical twine. One end of each muscle was anchored to the servomotor/transducer to record contractility dynamics.

IV. Main Experiment

Testing began after the EDL muscles had been quiescent and were in a fully unpotentiatied state prior to the experiment. Specimens shortened from 1.10 to 0.90 L_O while speeds were set from 0 (isometric) to 0.70 of maximum shortening velocity (Vmax) for each test contraction. Shortening speeds were tested at ~0.70 Vmax for concentric contractions. The first and last contraction of each frequency series was always done at 0 Vmax (isometric). Following the first concentric contraction the muscle underwent four brief (100 Hz, 400 msec) conditioning stimuli over 10 seconds to induce near maximum levels of potentiation (CS) with little fatigue. The experimental protocol was then repeated with the muscle now in a posttetanic state (Figure 7). Active force was found by examining the difference between the total and passive forces during the active and passive down ramps (Figure 8). In order to retain integrity and minimize fatigue, a rest period of 20 minutes was allowed between each frequency series. Comparisons of NME (Total concentric work/ # of pulses) were made between the potentiated and unpotentiated state at each frequency. Relative force potentiation was recorded as a ratio of final force to initial force. Rate of force development values (+DP/dt) were manually determined from the peak of the most rapid pulse.

Following the experimental protocol muscles were rapidly frozen utilizing liquid nitrogen cooled tongs and were stored at -80° C. Control muscles were frozen ~20 minutes after testing to minimize residual potentiation while conditioned muscles received a final CS procedure and frozen ~20 seconds afterwards.

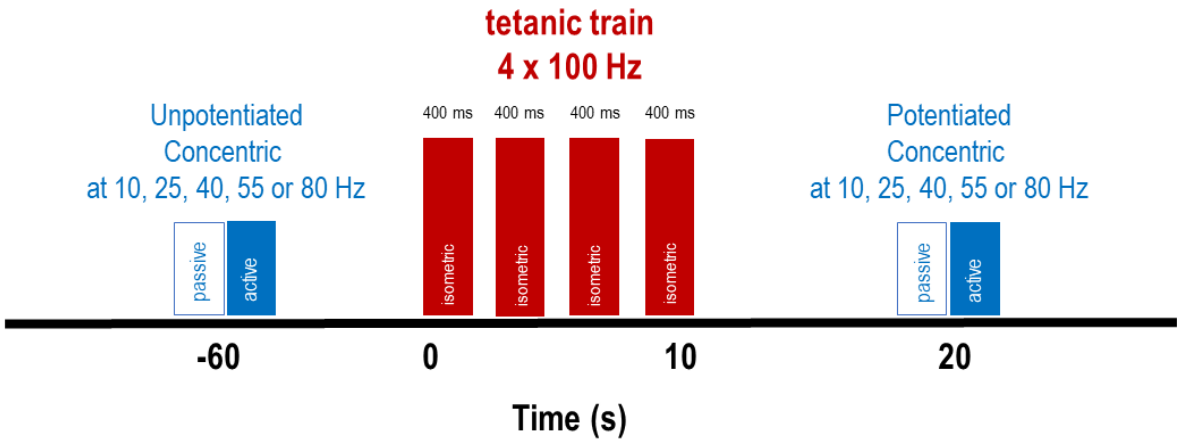

Figure 7: Main experimental procedure schema. Muscles were subjected to concentric contractions at various frequencies in randomized order (10, 25, 40, 55, and 80 Hz) while muscle shortening occurred (1.10 to 0.90 L_O, ~70% Vmax). Measurements were taken during the shortening phase of the contraction before and after the conditioning stimulus (4 x 100 Hz, 400 msec, over 10 seconds). Stimulus timing remained consistent for all frequency trials.

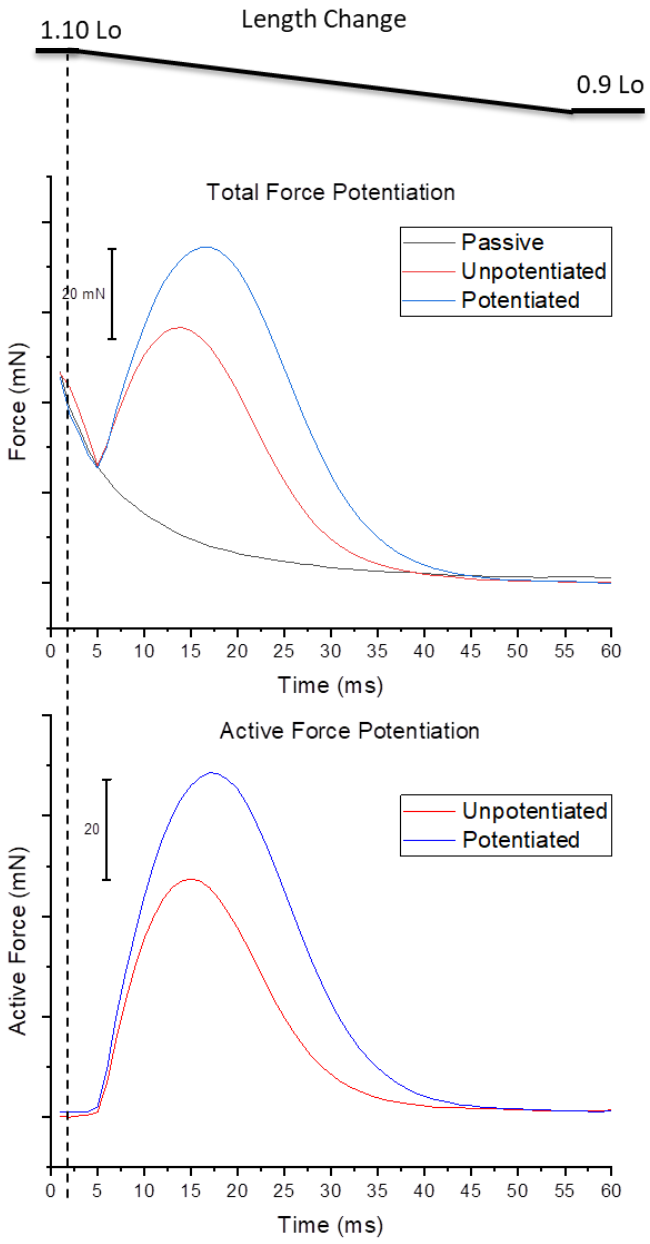

Figure 8: Potentiation of active concentric force. The concentric movement of the muscle produces some levels of innate tension possibly due to the series elastic components and uneven shortening of sarcomeres. A mock contraction, or passive ramp, is used to simulate the changes in tension independent of stimulated contraction. Calculating the difference between the stimulated and blank traces provide the active force response generated by the EDL.

V. Statistical Analysis

Initially data were checked for outliers and distribution using Shapiro-Wilks normality tests within each frequency (10, 25, 40, 55, or 80 Hz). The effect of the conditioning stimulus on absolute contractile values (Force, Work, NME; Pre & Post CS) was investigated with a two-tailed paired student T-test at each frequency for both genotypes. Relative potentiation of NME (Pre/Post) was tested using a two-way mixed measures ANOVA to investigate the main effects of frequency (10, 25, 40, 55, or 80 Hz) and genotype (Wild type or skMLCK$^{-/-}$). Post-hoc analyses were evaluated with a Bonferoni correction. All statistical analysis was done utilizing SPSS (Statistical Package for the Social Sciences v.28). Significance levels are set at $p<0.05$. All data are reported as mean ± SEM.

Some relative NME data were found to violate the assumption of sphericity (X^2 (9) = 21.44, P= 0.012) so Greenhouse-Geisser values were used. When checked for t-test assumptions it was found that skMLCK$^{-/-}$ rate of force development values were not normally distributed within each frequency. A one-tailed Mann-Whitney rank sum test was used as a non-parametric alternative to examine the relative effect of potentiation on the rate of force development between wild type and skMLCK$^{-/-}$ EDLs.

Chapter Five: Results

During all experiments measurements of concentric force (mN) and work (Δ mm* mN) were taken during ramp shortening (from 1.10 -> 0.90 L_o, ~70% Vmax). During the contraction muscles were stimulated at one of 5 frequencies (10 to 80 Hz) both before and after a potentiating stimuli train (4x 400ms 100 Hz, over 10s). All stimuli were administered at the same starting time point during the shortening phase of the concentric down ramp. A consequence of our fast ramp time was that the window available for stimulating muscles was very brief. As a result, our 10, 25, 40, 55 and 80 Hz protocols allowed for approximately 1,2,2,3 and 4 individual pulses during both the pre- and post-ramps and all determinations of force, work and efficiency are based on these (both genotypes). Incomplete pulses were included in calculations as a fraction relative to the duration of completed pulses so that all data remained concentric. Force data will be presented first followed by work and then efficiency.

I. PTP Induced Force Enhancement

Total force output (mN) was recorded from the active tension generated by the EDLs during contraction trials. Active force was calculated as the difference in tension between the total and passive down ramps (Figure 8). The effect of PTP induced force enhancement was observed from peak force values before and after the CS. Representative traces of active concentric force at every frequency are presented in figure 9. A two-tailed paired student t-test determined that absolute peak concentric force was significantly potentiated following the CS at all frequencies for both genotypes (N= 12, $P<0.05$). Data showing effects of potentiation on absolute peak concentric force are presented in table 1. Relative concentric force, which was investigated with a two way mixed measures ANOVA (Frequency x Genotype), revealed greater

in wild type EDLs (57% max) compared with skMLCK$^{-/-}$ (20% max) EDLs at every frequency (P< 0.05, Figure 10).

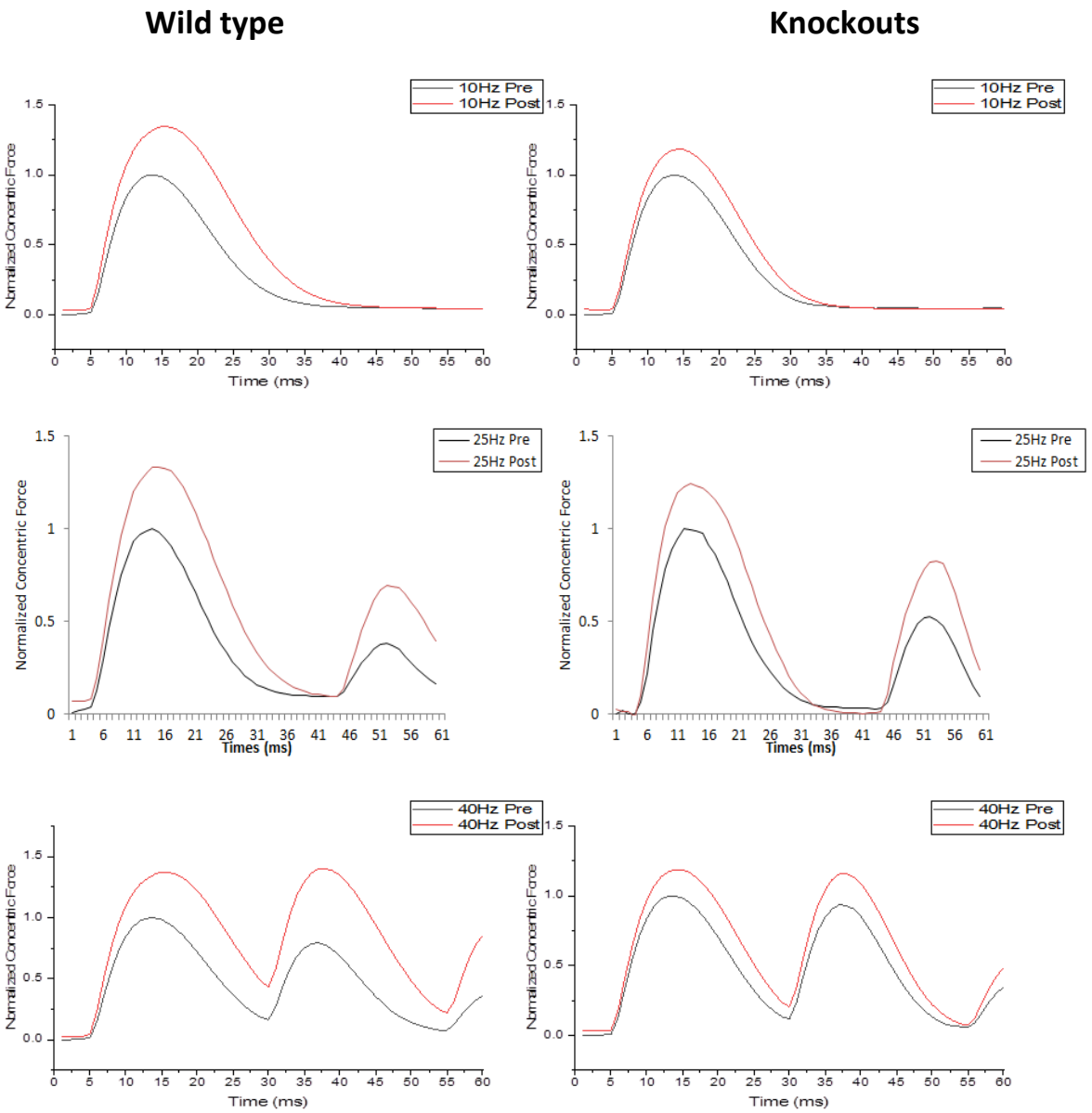

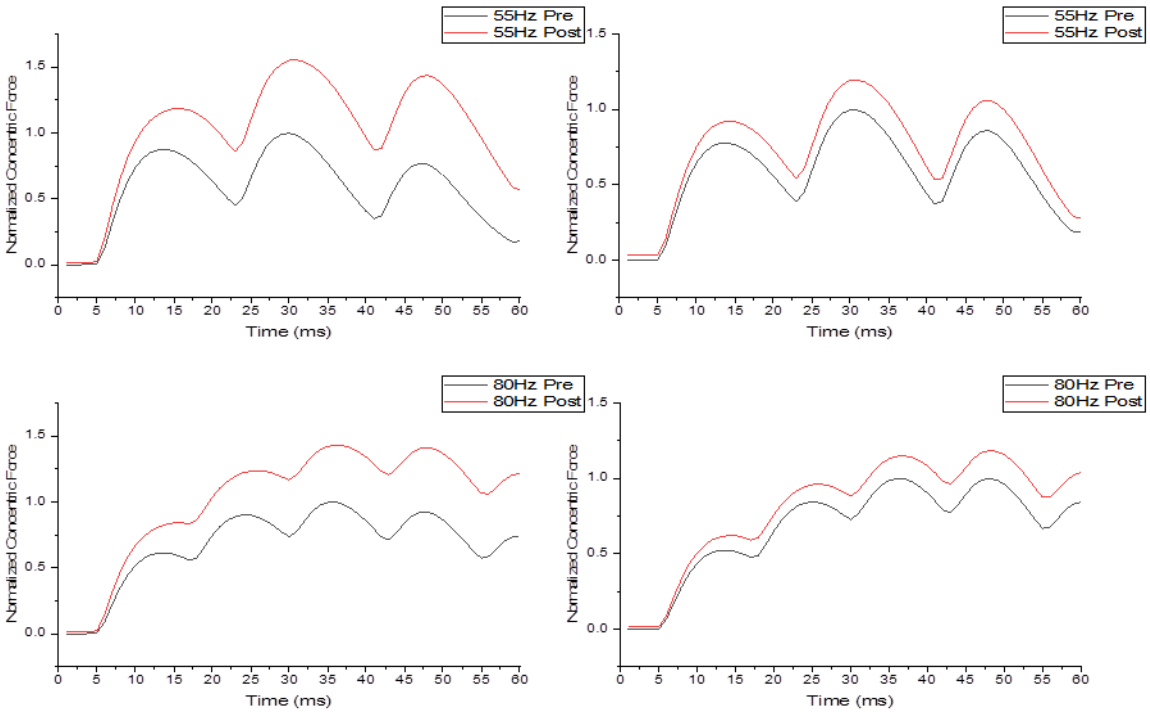

Figure 9: Active concentric force before and after the conditioning stimulus at various frequencies (10 Hz, 40 Hz, 55 Hz, and 80 Hz). 1.10 -> 0.90 L_o, ~70% Vmax. Data were collected throughout the duration of the shortening ramp.

Table 1: Effect of the conditioning stimulus on peak concentric force (mN) in mouse EDL

Force (mN)		Stimulus Frequency (Hz)				
Genotype		10 Hz	25 Hz	40 Hz	55 Hz	80 Hz
Wild type	Pre	14.23±0.78	14.20±0.69	13.73±0.73	15.91±1.17	22.38±1.95
	Post	19.44±1.01*	19.27±1.01*	20.01±1.18*	24.86±1.73*	32.44±2.39*
SkMLCK$^{-/-}$	Pre	12.42±1.16	12.57±1.16	12.90±1.01	16.50±1.40	24.36±2.17
	Post	14.77±1.29*	15.03±1.30*	15.33±1.22*	19.69±1.61*	28.37±2.60*

Values are means ± SEM, n = 12. Means with an * indicate means that were significantly impacted by the conditioning stimulus. $P < 0.05$

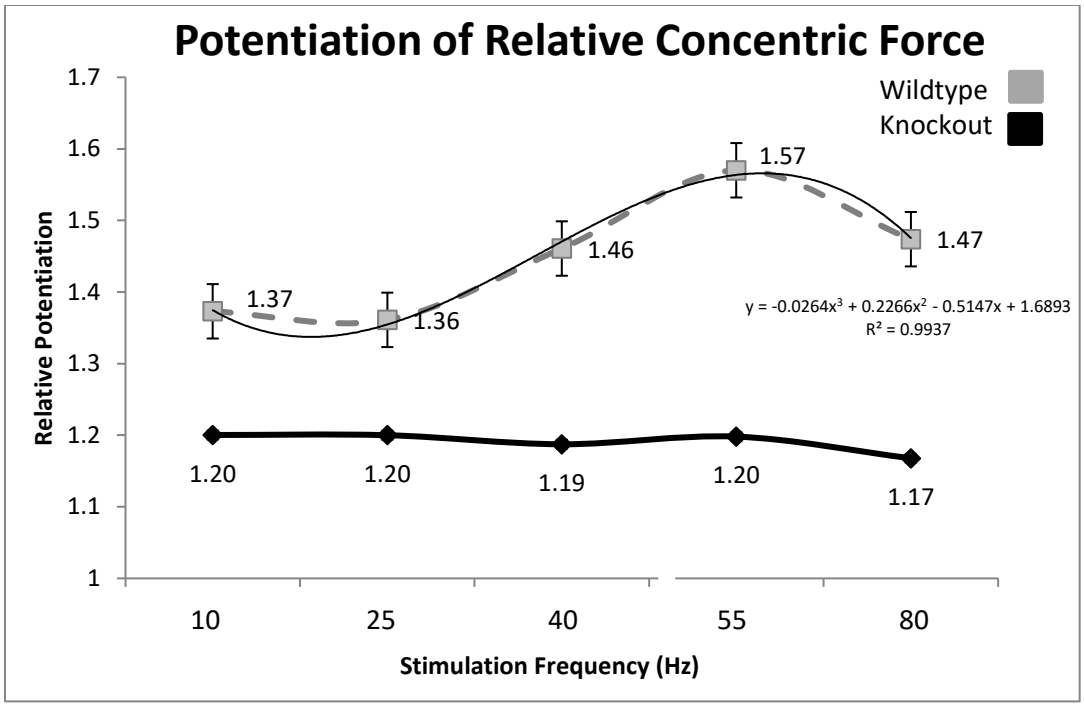

Figure 10: Relative potentiation of peak concentric force in wild type and skMLCK$^{-/-}$ EDLs. Knockout potentiation across frequencies was rather uniform while wild type potentiation was greater overall and specifically at higher frequencies. Relative values were calculated as Post/Pre.

2. PTP Induced Work Enhancement

A paired samples t-test determined that absolute work during the single applied pulse was significantly increased for both genotypes following the CS (P= 0.05, Figure 11). As expected the wild type EDLs displayed a greater potentiation of work than the skMLCK knockout cohort (i.e. WT 64%, KO 30%). A one tailed independent samples t-test indicated that concentric output preceding the CS was not significantly different between wild type and knockouts t(22) = 1.022, P = 0.159 (Figure 11). Indeed, no significant differences of pre-CS work values were found between genotypes at any frequency (Figure 12).

3. Effect of Stimulus Frequency

Higher stimulus frequencies produced multiple pulses from which total work was calculated (mm*mN). The results of a two-tailed paired samples t-test revealed significant improvement in absolute work post-CS at every tested frequency ($P<0.001$, Table 2). As expected WT EDLs with functional skMLCK had much greater magnitudes of mechanical enhancement (Peak 92%) compared to the knockout cohort (Peak 33%, Figure 13). Data describing influence of CS on absolute concentric work are presented in Table 2. The greatest amount of relative potentiation was observed during the 40 Hz trials and appears to diminish at higher frequencies (Figure 13). The knockout cohort displays substantial enhancement of work following the CS without skMLCK expression indicating the possibility of other mechanisms leading to skeletal muscle potentiation. The results demonstrate the effect of phosphorylation induced PTP on the augmentation of fast muscle contraction.

Table 2: The effect of a potentiating stimulus on total absolute work (mm*mN) in mouse EDL

		Stimulus Frequency (Hz)				
Genotype		10 Hz	25 Hz	40 Hz	55 Hz	80 Hz
Wild type	Pre	10.4 ±0.76	13.5 ±1.04	16.8 ±1.47	25.5 ±2.45	41.8 ±4.20
	Post	16.9 ±1.20*	22.4 ±1.72*	32.1 ±2.67*	45.8 ±3.93*	63.6 ±5.30*
SkMLCK$^{-/-}$	Pre	9.2 ±.0.87	11.8 ±1.14	16.5 ±1.55	27.5 ±0.53	47.7 ±4.07
	Post	11.8 ±1.07*	14.9 ±1.48*	21.9 ±2.07*	35.3 ±3.11*	55.8 ±4.75*

Work (mm * mN) was assessed from the force producing period of the concentric contraction during each stimulation (1.10 -> 0.90 L_o, ~70% Vmax). Values with an * indicate means that were significantly impacted by the conditioning stimulus. ($P < 0.05$) Values are means ± SEM, n = 12

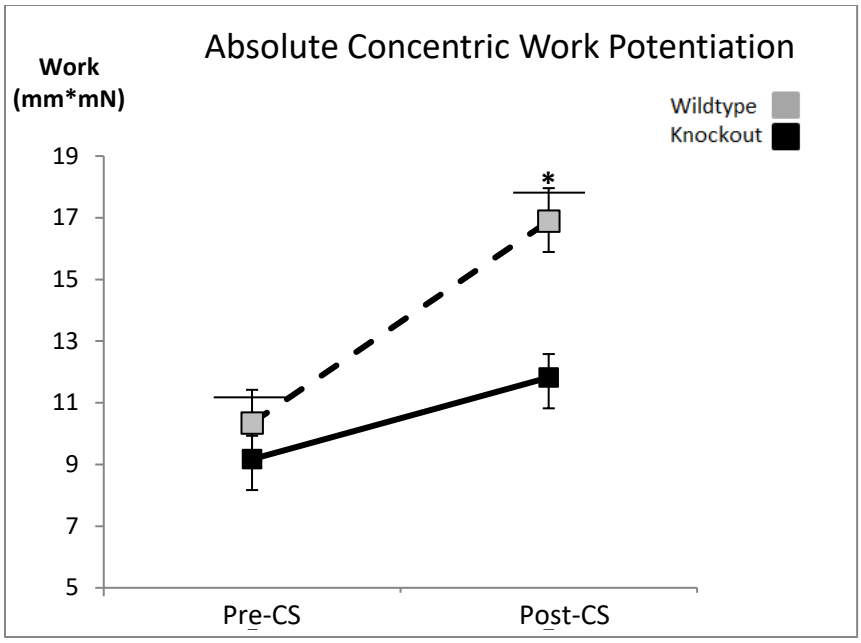

Figure 11: Potentiation of work during a single pulse. The 10 Hz trial was chosen as a single stimulus pulse was administered during contraction (1.10 -> 0.90 L_o, ~70% Vmax). Absolute work values were significantly increased by the conditioning stimulus in both genotypes (P= 0.05). However, a one-tailed independent t-test confirmed that pre-CS values were not significantly different from each other (P=0.318). Following induction of PTP wild type EDLs had a significantly higher magnitude of force potentiation than knockouts. n =12.

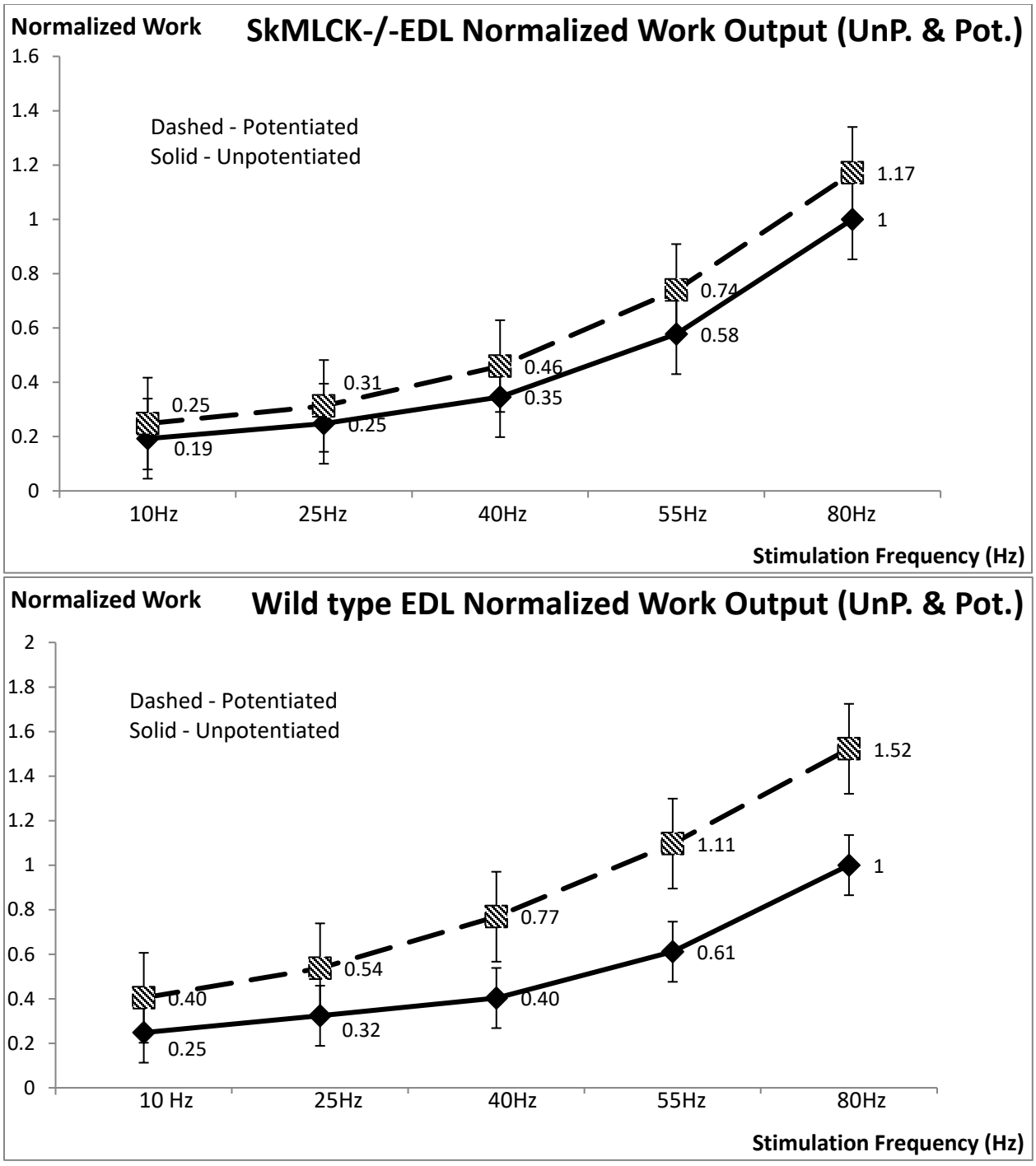

Figure 12: Normalized work output at five frequencies (10, 25, 40, 55, and 80 Hz) for Top.) Wild type. Bottom.) SkMLCK$^{-/-}$. Dashed lines represent data taken post CS compared to the solid line representing work before potentiation. Pre and post work values were normalized to the peak unpotentiated work value. Within the WT EDL, it can be seen that the potentiated 55Hz trial produced more work than the unpotentiated 80Hz trial. n = 12.

4. Neuromuscular Efficiency

Neuromuscular efficiency (NME) was calculated as a ratio of total work output (Δ mm*mN) to number of pulses during the force producing segment of the concentric down ramp. It was hypothesized that the conditioning stimuli would cause a significant increase in NME compared to before the CS. A two-tailed paired samples t-test revealed significant improvement of absolute NME at every tested frequency for both genotypes (P=<0.001). The WT genotype was expected to display higher levels of NME enhancement due to skMLCK presence as opposed to knockout EDLs. As expected the wild type cohort displayed significantly higher potentiation of relative NME compared to the skMLCK$^{-/-}$ group (P=<0.001, Figure 13). When collapsed across frequencies wild type EDLs displayed a range of increased relative potentiation values from 58-92% while knockouts displayed a range of 17-33% (Figure 13).The results of a two-way mixed measures ANOVA on relative NME revealed a significant interaction between frequency (10, 25, 40, 55, or 80 Hz) and skMLCK expression (Wild type & knockout) [F (4, 120) = 3.08, P = 0.0191]. The genotype of the EDL muscle significantly impacted the frequency dependent potentiation of contraction. SkMLCK expression combined with levels of frequency both contributed to impact relative NME. The greatest amount of NME potentiation was observed during the 40 & 55 Hz trials and decreased at higher frequencies trials (Figure 13). NME potentiation demonstrates that greater amounts of work are being done per individual stimuli pulse within a muscle. A greater work: pulse ratio following potentiation would represent greater efficiency during each motor neuron discharge.

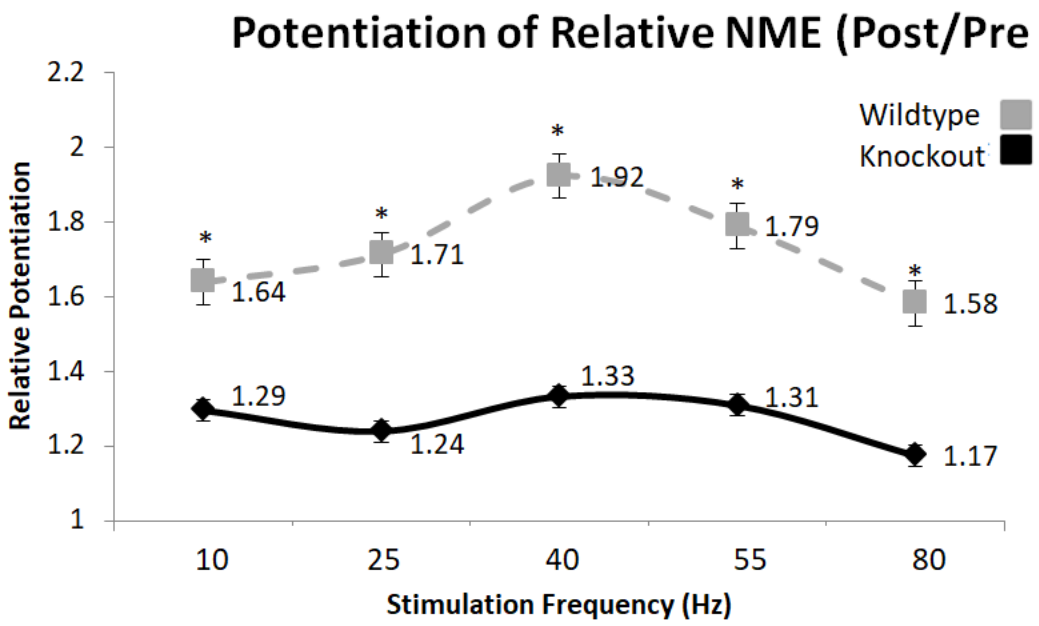

Figure 13: Comparison of relative NME potentiation during concentric contractions of wild type and skMLCK-/- EDLs. The wild type cohort consistently displayed significantly higher levels of relative potentiation at every frequency compared to the knockout cohort *, $P<0.05$. One can observe the highest amount of relative increase was during the 40 Hz trial in both genotypes. Stimuli were applied during concentric contractions (1.10 -> 0.90 L_o, ~70% Vmax).

5. Rate of force development

Peak rate of force development was manually evaluated from each series of concentric contraction traces. A two-tailed paired student t-test was used to investigate alterations in rates of force development before and following the CS. Significant improvement to RoFD was observed at every frequency within the wild type cohort ($P<0.001$). Within the skMLCK$^{-/-}$ EDLs rate of force development was significantly impacted at every frequency except 80 $Hz_{UnP\text{-}Pot}$

[t(11) = 2.003, p = 0.07]. The relative enhancement of RoFD (Post/Pre) following CS was also investigated (Table 3). When checked for standard assumptions it was found that multiple levels of skMLCK$^{-/-}$'s relative rate of force development data were not normally distributed. Thus, a Mann-Whitney U test was used to compare between genotypes within levels of frequency. Relative rate of force development was significantly higher in wild type EDLs compared to skMLCK$^{-/-}$ mice at 40 Hz (U = 140, Z = 3.926, P = 0.000), at 55 Hz (U = 131, Z = 3.406, P = 0.000), and at 80 Hz (U = 120, Z = 2.771, P = 0.005) (n = 24). There was no significant difference found between genotypes at the 10 & 25 Hz trials. The wild type EDLs appear to have conserved levels of potentiated RofD across all frequencies while the skMLCK$^{-/-}$ EDLs have comparable values only at low frequencies before declining at 55-80Hz (Table 3).

Table 3: The effect of the conditioning stimulus on relative rate of force development (dP/dt) (Post/Pre) in skMLCK$^{-/-}$ and wild type cohorts.

(Post/Pre, dP/dt)	Stimulus Frequency (Hz)				
Genotype	10 Hz	25 Hz	40 Hz	55 Hz	80 Hz
Wild type	1.66 ± 0.16^{a}	1.47 ± 0.09^{a}	1.46 ± 0.06^{a}	1.32 ± 0.05^{a}	1.36 ± 0.05^{a}
Knockout	1.55 ± 0.2^{a}	1.37 ± 0.09^{a}	1.16 ± 0.03^{b}	1.09 ± 0.03^{b}	1.11 ± 0.05^{b}

Values are means ± SEM, n = 24. Peak rate of force development (dP/dt) was measured during the shortening phase of the concentric contraction (mN*ms^{-1}). Superscripts denote significant differences between genotype means. The wild type cohort appears to retain levels of enhancement at higher frequencies compared to the skMLCK$^{-/-}$ cohort which are significantly lower at the same frequencies (40,55, & 80Hz). P<0.05

Chapter Six: Discussion

This study aimed to investigate the effect of RLC phosphorylation-mediated PTP on neuromuscular efficiency (Total concentric work: # of pulses) at five frequencies of stimulation (25^{o}C). The effects of PTP were investigated utilizing skMLCK ablated mice: a unique negative control for RLC phosphorylation-mediated potentiation. Significant enhancement of concentric work output was observed following the conditioning stimulus at every frequency for both genotypes. Wild type EDLs displayed substantially greater amounts of work potentiation compared to knockouts. Similarly, neuromuscular efficiency was significantly potentiated following the conditioning stimulus at every frequency for both genotypes. As hypothesized, the wild type cohort demonstrated significantly higher levels of NME potentiation (58-92%) compared to the knockouts levels of NME potentiation (17-33%) indicating that individual stimuli discharged are producing more force output compared to the same stimuli discharged in the unpotentiated state. The difference in potentiation values between genotypes was a consequence of myosin light chain kinase expression.

Concentric contractions were used because they elicit greater amounts of potentiation compared to isometric contractions and better represent natural movement (Vandenboom et al., 2013). Precursor frequency trials have previously been explored by Gittings et al., (2017) examining concentric potentiation (1.10 -> 0.90 Lo, 25°C). They demonstrated that potentiation of muscle force is shortening velocity dependent by utilizing various speeds of contraction (0.10, 0.30, 0.50 Vmax) at five frequencies (10, 25, 40, 70, and 100 Hz). Peak wild type force potentiation was observed during their fastest shortening velocity (0.50 Vmax) at the intermediate tested frequencies 25-45Hz. Our concentric contractions were conducted at a

higher Vmax (0.70) which produced optimal potentiation at the 40Hz frequency in both genotypes. In comparison with their most rapid speed of shortening (0.50 Vmax), our magnitude of force potentiation was slightly lower in the wild types (0.70 Vmax), but very similar in the knockout models. Our results agree with the Gittings et al. (2017), conclusion that faster shortening speeds increase the activation frequency at which concentric potentiation is maximal. The speed of shortening ramp we tested (1.10 -> 0.90 Lo, 70% Vmax) was more rapid than other studies; however this speed may better represent the normal operation range of murine skeletal muscle.

One can quantify the effective gain in the work-frequency relationship by making comparisons of the stimulation frequency required for 50% of maximal unpotentiated work between genotypes following PTP. The amount of 'gain' in frequency can estimate how much less stimulation is required in the potentiated state compared to the unpotentiated state for similar work outputs. In the wild type EDL the stimulation rate required for half maximal work output decreased from 48 -> 22Hz following potentiation compared to the knockout's $work_{50\%}$-frequency gain of 48 -> 40Hz. The amount of stimulation that is able to be conserved is higher in the wild type EDLs indicating that RLC-phosphorylation mediated potentiation has a significant influence. Within an intact neural system this may result in the effective conservation of stimulation or perhaps a lowering in perceived exertion.

As summarized by Hennig & Lomo (1987), alterations to the motor neuron pool control the gradation of muscle force in a pulse-dependent manner. It has previously been established that the magnitude of skeletal muscle potentiation is also stimulation frequency dependent as a direct consequence (Vandenboom, 2013). This phenomenon was apparent in our experiment's

wild type cohort displaying maximal levels of potentiation around the mid-range frequencies (40Hz) before decreasing at higher frequencies. On the other hand the knockout EDLs appeared to display no frequency dependence to potentiation at all; the primary factor of course being the ablation of skMLCK. It is known that at higher frequencies the amount of calcium released during contraction is elevated compared to lower frequency contractions (Westerblad et al., 1993). In terms of skeletal muscle potentiation this causes a reduced effectiveness of the increased calcium sensitivity provided from RLC-phosphorylation when calcium starts to become saturated. This explains why the EDL muscles displayed a peak amount of work and NME enhancement at the mid-range of the tested frequencies. This phenomenon also illustrates the calcium related ceiling effect for RLC-mediated potentiation. Comparisons between multiple studies are difficult because the normal firing rate, firing patterns, and fibre recruitment patterns observed in fast murine skeletal muscle may not be represented in other species or even other muscle groups.

The influence of skeletal muscle potentiation on contractile economy has been investigated previously from our lab. Bunda, J., (2018) investigated the fluctuation of contraction metabolites (ATP, RLC-P, PCr, Lactate) before and after inducing staircase potentiation. Their investigation of metabolic efficiency utilized the same EDL cohorts as our study. Following potentiation it was found that wild type EDLs generated 44% greater force than skMLCK$^{-/-}$ muscles without the increased use of ATP (Bunda, J., 2018). Metabolite economy was demonstrated to be another aspect of contractile efficiency that is significantly impacted by skeletal muscle potentiation. In contrast earlier work Abbate et al., (2001) concluded that RLC-phosphorylation mediated potentiation instead reduced the economy of

contraction. They reported that PTP increased the energetic requirements for contraction in comparison with the unpotentiated state which is in contradiction to many labs' data. However the results from Abbate et al. (2001), were procured from a rat *gastrocnemius* model *in situ* as opposed to mouse EDL which makes comparisons difficult. Another key difference was their ability to stimulate their muscle directly through the severed sciatic nerve which may produce alternative recruitment patterns and stimulation timings compared to our method of whole muscle activation. It was unclear whether the increased metabolic energy costs post CS were simply due to more work output by the muscle or were a characteristic of potentiation (Abbate et al., 2001). The conflicting result may be explained by Barclay & Lewis (2014), who demonstrated that low levels of thin filament activation reduced contraction efficiency possibly just due to fewer numbers of cycling cross-bridges.

Previous studies that have attempted to measure mechanical contraction efficiency *in vivo* have utilized alternate methods of quantification. Research groups like Lewis & Barclay (2005, 2014) and Smith et al., (2011) have incorporated the enthalpy output of the muscle in relation to work generation to quantify the change in efficiency. Their results demonstrated that the mechanical efficiency of WT EDL and soleus muscles was relatively lower at low frequencies (40Hz) compared to high frequency stimulation (160Hz). They showed that the level of fibre activation within the test muscle is integral the amount of mechanical efficiency, and also note the increased saturation of calcium at high frequency contraction causes an effect. Other groups that have attempted to study efficiency changes *in vivo* have often been attempted with forms of electromyography (EMG), which are beneficial for observing whole muscle function (Smith et al., 2005,2011). However the measurement of contraction

parameters in this manner does not allow one to observe changes at the level of the muscle fibre. Variations in muscle fibre composition and discharge rate patterns make electromyography conclusions relative to whole muscle function. Early forms of surface EMG also had reliability problems in discerning individual motor unit firing patterns due to amplitude cancellation and other confounding variables (Christie et al., 2009).

During prolonged contractions the normal pattern of motor neuron discharge in humans involves an initial decrease in rate before later rising to normal levels. This has been referred to as the triphasic pattern of motor unit discharge and was initially thought to be a fatigue-induced response to stimulation (Woods et al., 1987). However De Luca (2005), was able to show that the depression of firing rates following potentiation still occurred in fatigue independent contractions. They noted that the timing of the MUDR depression coincided with the induction of potentiation, and that the causation of reduced firing rates may come from some neural influence instead. Several human studies have since used an *in situ* approach to measure rate coding output from the intact motor neuron following potentiation. Inglis et al. (2011), demonstrated a significant decrease (9.8%) in motor neuron discharge rates following PAP in human *tibialis anterior* muscle. Another human potentiation study from Klein et al., (2001), showed similar results in a substantial 1-6 Hz decline in rate coding during MVC following tetanic contraction. In both studies there was significant depression of firing rate whilst twitch force was still characteristically enhanced. Their results demonstrated that potentiation and the neural control of motor neuron function have significant interactions in the intact neuromuscular system.

The teleological purpose behind this interaction within an intact neural system has not been fully elucidated, but it has been subject to speculation. Recently a review by Rice, C. & Zero, A. (2021), summarized the current understanding of the relationship between human PAP and neural activation. The CNS-directed response to PAP appears to include a significant depression of rate coding and general down regulation of neural responses (Klein et al., 2001; Inglis et al., 2011; Zero & Rice A., 2021). During a prolonged or high intensity contraction this conserved activation may work to lower the computational load on the CNS compared to the unpotentiated state. This could in turn delay or minimize the effects of fatigue in skeletal muscle while still simultaneously providing the characteristic enhancement of force output. A possible mechanism involves the motor neuron pool receiving an excitatory drive from the CNS that initially decreases firing rate to compensate for potentiation of muscle force before later increasing to compensate for the effects of fatigue (De Luca 2005). Another consideration could be the preservation of the enhanced calcium sensitivity provided from potentiation. A reduced requirement for stimulation following potentiation would cause a lower overall discharge rate and subsequent lesser amounts of calcium release. This would possibly function to conserve the magnitude of potentiation's effect on calcium sensitivity at high stimulation frequencies.

During normal locomotion muscle fibres are repeatedly shortened and lengthened which requires dynamic control over the involved motor units. One of the most common types of contractions during regular movement in humans involves the coupling of eccentric lengthening with concentric shortening in what is known as the stretch-shortening cycle. Interestingly, this coupling of movements result in increased work, force, and power compared to contractions without an initial lengthening motion (Cavana et al., 1965). Skinned fibre studies

have established the responsible mechanism behind the eccentric portion enhancement as non-crossbridge viscoelastic elements, mainly the structural protein titin (Tomalka et al., 2020). The changing of muscle length throughout a concentric contraction introduces the possible aspect of length dependence to the force-potentiation relationship. However the Xeni et al., (2011), group showed no length dependence of potentiation in concentric contractions suggesting that the instantaneous changes in muscle length interact with shortening velocity to modulate the potentiation response.

It is generally known that the amount of *isometric* potentiation that can be elicited in skeletal muscle is higher at shorter lengths compared to longer lengths (Rassier, D. 2008). However at the beginning of the shortening phase of a concentric contraction it appears that potentiation is greatest before declining based on the *time course* that the muscle shortens (Grange et al., 1998)**.** While this is occurring, there are simultaneous adjustments to the neural scheme controlling motor unit discharge rate throughout the contraction (Klein et al., 2001,2002; Inglis et al., 2011). There may be significant interactions of these characteristics that may synergistically allow for optimal generation and extended maintenance of force. The induction of potentiation in muscle it seems to temporally coincide with the neural depression seen by Rice & Zero (2021), as well as that the force requirement for stimulation decreases. The phenomenon could indicate a lower influence of PTP on MUDR during the initial shortening shown by depressed firing rates. However as the muscle continues to shorten the motor unit firing rates begin to rise as the levels of force potentiation begin to decrease (Klein et al., 2001; Inglis et al., 2011). The precise interactions of length dependent force potentiation and motor unit discharge rate have not been previously explored and remain an area of interest. In

consideration of whole system function these interactions appear to be by design trade-offs as opposed to physiological coincidence During the lengthening phase of skeletal muscle contraction potentiation is non-existent, but it is known that already potentiated muscles have slower relaxation rates (Xeni et al., 2011). It may be worthwhile to investigate the firing rate response in potentiated eccentric contractions.

The clear presence of potentiation in knockout EDLs without the expression of skMLCK indicates the possibility of RLC-phosphorylation independent mechanisms leading to enhancement of mechanical output. Work by Smith et al., (2013), previously investigated alternative mechanisms within fast lumbrical muscles which do not display RLC phosphorylation at all due to fibre composition. The remaining potentiation observed was ascribed to elevations in resting myoplasmic Ca^{2+} concentrations following tetanic stimulation. The increased saturation of Ca^{2+} buffering systems and promotion of Ca^{2+}-troponin binding works to increase the Ca^{2+} sensitivity of following contractions (Smith et al., 2013). Other unknown factors such as non-specific kinases may still contribute to the enhancement of force observed in skMLCK$^{-/-}$ skeletal muscle. Since RLC-phosphorylation is the primary mechanism leading to PTP then one must assume the differences in relative potentiation between genotypes following the CS are indeed due to the expression of skMLCK (Vandenboom et al., 2013).

The *in vitro* method used to measure contraction efficiency has some advantages over *in situ* approches. Utilizing isolated skeletal muscle allows for the control of factors such as fibre type, temperature, shortening speeds, etc. that cannot be easily simulated in other environments (Vandenboom et al., 2013). Our setup allowed for consistent stimulation timing and specific frequency administration that is ideal for measuring the responsive characteristics

of the whole muscle. However when a muscle is excised it is also isolated from the neuromuscular system. As such, our model lacked the afferent signals and neural influences that one would see in an intact neuromuscular system. One would expect to see variations in stimulation timings and recruitment patterns within *in situ* models. The supramaximal stimulation used to activate the homogenous type IIX/B EDL fibres *in vitro* may be a better representation of single motor unit function *in vivo* (MacIntosh, 2010). Our *in vitro* setup also allowed for the control of temperature throughout the experiment. This is important because at physiological temperatures the range of potentiation values is variable (MacIntosh, 2010). It was observed that at room temperature and lower myosin filaments became significantly disarrayed compared to higher temperatures (Xu et al., 2003). This allowed the myosin S1 head to have greater mobility at low temperatures compared to the orderly arrangement seen at physiological temperatures. This temperature reliance can explain why RLC-phosphorylation has less of an effect on Ca^{2+} sensitivity at low compared to physiological temperatures (Xu et al., 2003; MacIntosh, 2010)

Significance

Previous research has revealed much about how RLC phosphorylation-meditated potentiation affects contraction. Posttetanic potentiation has primarily been known to augment force output following tetanic stimulus, but clearly it has the potential of influencing other dynamics of contraction to modulate muscle force output. Human studies have shown that PAP reduces rate coding *in situ*, and can influence contraction at the level of the motor neuron. Our study investigated the effect of PTP on the NME gained for each pulse during concentric

contractions *in vitro*. The effect was observed with the use of unique skMLCK$^{-/-}$ mice providing EDL muscles that acted as a negative control for potentiation. The potentiation of NME observed in the EDL muscles showed how PTP interacts with other parameters of contraction. The purpose of this interaction may be for compensatory purposes during normal function. PTP may influence neural pathways that are not apparent without an intact neuromuscular system which provides warrant for further investigation.

Limitations

There are limitations of this experiment that must be addressed. Firstly, each muscle excised from the test animals was assumed to be similar in size and fibre type composition. The EDL was an appropriate model to use due to its small size and uniform composition high in fast type IIb fibres (Gittings et al., 2011). This feature allows for sustained muscle viability *in vitro* through sufficient oxygenation and nutrients delivery via diffusion (Barclay, 2005). Use of larger muscle groups may present problems with fibre viability over extended durations.

The specific lineages of skMLCK ablated mice were first developed at Brock University in 2005, and have been maintained through genealogical control ever since. Compared to earlier studies our current generations of knockout mice are consistently displaying slightly elevated levels of potentiation in similar fast skeletal muscle (Gittings et al., 2007, 2013; Xeni et al., 2011). The limitation that must be addressed is the incomplete ablation of the MYLK2 gene leading to partial skMLCK-mediated potentiation in the knockout models. The causation of this could be potential genetic drift over time and inbreeding within the colony.

The experiments using isolated skeletal muscle from different genotypes allowed us to assess the mechanistic basis of change in neuromuscular efficiency, (i.e. RLC phosphorylation versus other) but are a poor surrogate for the intact neuromuscular system. As Zero & Rice (2021), reviewed the influence of potentiation of the neural scheme of muscle control is relatively understudied. From our experiment we can infer that the muscle function observed during the *in vitro* experiments applies *in vivo*. Any dynamic interaction of neural based force modulation and skeletal muscle potentiation would have to be examined within an intact neuromuscular system.

Due to time related constraints and COVID restrictions we were unable to proceed with myosin RLC-phosphorylation quantification. However previous experiments from our lab have previously quantified potentiation levels in WT & KO EDL. Comparisons of relative potentiation values are difficult as factors such as muscle length, shortening speed, and temperature all influence the degree of RLC-phosphorylation. Grange et al. (1998), explored how low frequency stimulation (5Hz, 20s) impacted concentric work across three length excursions: 0.6, 1.2, and 1.6 mm (~5, 9, and 13% optimal muscle length) *in vitro 25C*. Their results indicated a 3.7-fold increase in phosphorylated RLC content (0.19 to 0.70 mol phosphate/mol RLC) (Grange et al., 1998). The Xeni et al. (2011), group which used concentric contractions demonstrated that stimulation at 2.5, 5, and 100-Hz elevated RLC phosphorylation from 0.16 ± 0.02 (rest) to 0.29 ± 0.03, 0.45 ± 0.02 and 0.56 ± 0.02 mol phos per mole RLC, respectively. We expected similar amounts of RLC-phosphorylation within our EDL muscles and that a significant relationship with potentiated force would be present.

References:

Abbate, F., Sargeant, A. J., Verdijk, P. W. L., & De Haan, A. (2000). Effects of high-frequency initial pulses and posttetanic potentiation on power output of skeletal muscle. *Journal of Applied Physiology*, *88*(1), 35-40.

Abbate, F., Van Der Velden, J., Stienen, G. J. M., & De Haan, A. (2001). Post-tetanic potentiation increases energy cost to a higher extent than work in rat fast skeletal muscle. *Journal of Muscle Research & Cell Motility*, *22*(8), 703-710.

Adam, A., & De Luca, C. J. (2003). Recruitment order of motor units in human vastus lateralis muscle is maintained during fatiguing contractions. *Journal of neurophysiology*, *90*(5), 2919-2927.

Adam, A., & De Luca, C. J. (2005). Firing rates of motor units in human vastus lateralis muscle during fatiguing isometric contractions. *Journal of Applied Physiology*, *99*(1), 268-280.

Alamo, L., Wriggers, W., Pinto, A., Bártoli, F., Salazar, L., Zhao, F. Q., ... & Padrón, R. (2008). Three-dimensional reconstruction of tarantula myosin filaments suggests how phosphorylation may regulate myosin activity. *Journal of molecular biology*, *384*(4), 780-797.

Barss, T. S., Ainsley, E. N., Claveria-Gonzalez, F. C., Luu, M. J., Miller, D. J., Wiest, M. J., & Collins, D. F. (2018). Utilizing physiological principles of motor unit recruitment to reduce fatigability of electrically-evoked contractions: a narrative review. *Archives of physical medicine and rehabilitation*, *99*(4), 779-791.

Bernhard, C. G., Euler, U. S. V., & Skroglund, C. R. (1941). Post-tetanic Action Potentials in Mammalian Muscle. Acta Physiologica Scandinavica, 2(3-4), 284–288.

Bickel, C. S., Gregory, C. M., & Dean, J. C. (2011). Motor unit recruitment during neuromuscular electrical stimulation: a critical appraisal. *European journal of applied physiology*, *111*(10), 2399.

Binder-Macleod, S. A., & Barrish, W. J. (1992). Force response of rat soleus muscle to variable-frequency train stimulation. *Journal of neurophysiology*, *68*(4), 1068-1078.

Binder, M. D., Heckman, C. J., & Powers, R. K. (2010). The physiological control of motoneuron activity. *Comprehensive physiology*, 3-53.

Bowslaugh, J., Gittings, W., & Vandenboom, R. (2016). Myosin light chain phosphorylation is required for peak power output of mouse fast skeletal muscle in vitro. *Pflügers Archiv-European Journal of Physiology*, *468*(11), 2007-2016.

Brown, I. E., & Loeb, G. E. (1998). Post-activation potentiation—a clue for simplifying models of muscle dynamics. *American zoologist*, *38*(4), 743-754.

Brunello, E., Caremani, M., Melli, L., Linari, M., Fernandez-Martinez, M., Narayanan, T., ... & Reconditi, M. (2014). The contributions of filaments and cross-bridges to sarcomere compliance in skeletal muscle. *The Journal of physiology*, *592*(17), 3881-3899.

Buller, A. J., Kean, C. J. C., Ranatunga, K. W., & Smith, J. M. (1981). Post-tetanic depression of twitch tension in the cat soleus muscle. *Experimental neurology*, *73*(1), 78-89.

Bunda, J., Gittings, W., & Vandenboom, R. (2018). Myosin phosphorylation improves contractile economy of mouse fast skeletal muscle during staircase potentiation. *Journal of Experimental Biology*, *221*(2).

Burke, R. E., Rudomin, P., & Zajac, F. E. (1970). Catch property in single mammalian motor units. *Science*, *168*(3927), 122-124.

Burke, R. E., Levine, D. N., Tsairis, P., & Zajac Iii, F. E. (1973). Physiological types and histochemical profiles in motor units of the cat gastrocnemius. *The Journal of physiology*, *234*(3), 723-748.

Burke, R. E., Rudomin, P., & Zajac Iii, F. E. (1976). The effect of activation history on tension production by individual muscle units. *Brain research*, *109*(3), 515-529.

Caterini, D., Gittings, W., Huang, J., & Vandenboom, R. (2011). The effect of work cycle frequency on the potentiation of dynamic force in mouse fast twitch skeletal muscle. *Journal of Experimental Biology*, *214*(23), 3915-3923Decostre, V., Gillis, J. M., & Gailly, P. (2000). Effect of adrenaline on the post-tetanic potentiation in mouse skeletal muscle. *Journal of Muscle Research & Cell Motility*, *21*(3), 247-254.

Cavagna, G. A., Saibene, F. P., & Margaria, R. (1965). Effect of negative work on the amount of positive work performed by an isolated muscle. *Journal of applied physiology*, *20*(1), 157-158.

Celichowski, J. (2005). The tetanic depression in unfused tetani of fast motor units in mammalian muscle. *Biocybernetics and Biomedical Engineering*, *25*(4), 27-35.

Celichowski, J., Dobrzyńska, Z., Łochyński, D., & Krutki, P. (2011). The tetanic depression in fast motor units of mammalian skeletal muscle can be evoked by lengthening of one initial interpulse interval. *Experimental brain research*, *214*(1), 19.

Chew, M. W. K., & Squire, J. M. (1995). Packing of α-helical coiled-coil myosin rods in vertebrate muscle thick filaments. *Journal of structural biology*, *115*(3), 233-249.

Close, R., & Hoh, J. F. Y. (1969). Post-tetanic potentiation of twitch contractions of cross-innervated rat fast and slow muscles. *Nature*, *221*(5176), 179-181.

Colson, B. A., Gruber, S. J., & Thomas, D. D. (2012). Structural dynamics of muscle protein phosphorylation. *Journal of muscle research and cell motility*, *33*(6), 419-429.

Colson, B. A., Locher, M. R., Bekyarova, T., Patel, J. R., Fitzsimons, D. P., Irving, T. C., & Moss, R. L. (2010). Differential roles of regulatory light chain and myosin binding protein-C phosphorylations in the modulation of cardiac force development. *The Journal of physiology*, *588*(6), 981-993.

Craig, R., & Padrón, R. (2004). Molecular structure of the sarcomere. *Myology*, *3*, 129-144.

Craig, R., & Woodhead, J. L. (2006). Structure and function of myosin filaments. *Current opinion in structural biology*, *16*(2), 204-212.

De Luca, C. J., Kline, J. C., & Contessa, P. (2014). Transposed firing activation of motor units. *Journal of neurophysiology*, *112*(4), 962-970.

De Luca, C. J., & Contessa, P. (2012). Hierarchical control of motor units in voluntary contractions. *Journal of neurophysiology*, *107*(1), 178-195.

De Luca, C. J., & Contessa, P. (2015). Biomechanical benefits of the onion-skin motor unit control scheme. *Journal of biomechanics*, *48*(2), 195-203.

De Luca, C. J., & Erim, Z. (1994). Common drive of motor units in regulation of muscle force. *Trends in neurosciences*, *17*(7), 299-305.

De Luca, C. J., Foley, P. J., & Erim, Z. E. Y. N. E. P. (1996). Motor unit control properties in constant-force isometric contractions. *Journal of neurophysiology*, *76*(3), 1503-1516.

De Luca, C. J., & Hostage, E. C. (2010). Relationship between firing rate and recruitment threshold of motorneurons in voluntary isometric contractions. *Journal of neurophysiology*, *104*(2), 1034-1046.

Dideriksen, J. L., & Farina, D. (2013). Motor unit recruitment by size does not provide functional advantages for motor performance. *The Journal of physiology*, *591*(24), 6139-6156.

Ding, J., Storaska, J. A., & Binder-Macleod, S. A. (2003). Effect of potentiation on the catchlike property of human skeletal muscles. *Muscle & nerve*, *27*(3), 312-319.

Duggal, D., Nagwekar, J., Rich, R., Midde, K., Fudala, R., Gryczynski, I., & Borejdo, J. (2014). Phosphorylation of myosin regulatory light chain has minimal effect on kinetics and distribution of orientations of cross bridges of rabbit skeletal muscle. *American Journal of Physiology-Regulatory, Integrative and Comparative Physiology*, *306*(4), R222-R233.

Eccles, J. C., Eccles, R. M., & Lundberg, A. N. D. A. (1958). The action potentials of the alpha motoneurones supplying fast and slow muscles. *The Journal of physiology*, *142*(2), 275-291.

Ennion, S., Pereira, J. S. A., Sargeant, A. J., Young, A., & Goldspink, G. (1995). Characterization of human skeletal muscle fibres according to the myosin heavy chains they express. *Journal of Muscle Research & Cell Motility*, *16*(1), 35-43.

Enoka, R. M. (2005). Central modulation of motor unit activity. *Medicine and science in sports and exercise*, *37*(12), 2111.

Enoka, R. M. (1995). Morphological features and activation patterns of motor units. *Journal of clinical neurophysiology: official publication of the American Electroencephalographic Society*, *12*(6), 538-559.

Enoka, R. M., & Duchateau, J. (2017). Rate Coding and the Control of Muscle Force. *Cold Spring Harbor perspectives in medicine*, *7*(10).

Farina, D., Negro, F., Muceli, S., & Enoka, R. M. (2016). Principles of motor unit physiology evolve with advances in technology. *Physiology*, *31*(2), 83-94.

Ford, L. E., Huxley, A. F., & Simmons, R. M. (1981). The relation between stiffness and filament overlap in stimulated frog muscle fibres. *The Journal of physiology*, *311*(1), 219-249.

Frazão, M., da Cruz Santos, A., Araújo, A. A., Romualdo, M. P., de Mello, B. L. C., Jerônimo, G. G., ... & do Socorro Brasileiro-Santos, M. (2021). Neuromuscular efficiency is impaired during exercise in COPD patients. *Respiratory Physiology & Neurobiology*, *290*, 103673.

Gallagher, P. J., Herring, B. P., & Stull, J. T. (1997). Myosin light chain kinases. *Journal of Muscle Research & Cell Motility*, *18*(1), 1-16.

Garland, S. J., & Griffin, L. (1999). Motor unit double discharges: statistical anomaly or functional entity?. *Canadian Journal of Applied Physiology*, *24*(2), 113-130.

Gittings, W., Huang, J., Smith, I. C., Quadrilatero, J., & Vandenboom, R. (2011). The effect of skeletal myosin light chain kinase gene ablation on the fatigability of mouse fast muscle. *Journal of muscle research and cell motility*, *31*(5-6), 337-348.

Gittings, W., Stull, J. T., & Vandenboom, R. (2016). Interactions between the catch like property and posttetanic potentiation of mouse skeletal muscle. *Muscle Nerve*, *54*(2), 308-316.

Gittings, W., Bunda, J., & Vandenboom, R. (2017). Shortening speed dependent force potentiation is attenuated but not eliminated in skeletal muscles without myosin phosphorylation. *Journal of Muscle Research and Cell Motility*, *38*(2), 157-162.

Gittings, W., Bunda, J., & Vandenboom, R. (2018). Myosin phosphorylation potentiates steady-state work output without altering contractile economy of mouse fast skeletal muscles. *Journal of Experimental Biology*, *221*(2), jeb167742.

Gordon, A. M., Homsher, E., & Regnier, M. (2000). Regulation of contraction in striated muscle. *Physiological reviews*, *80*(2), 853-924.

Grange, R. W., Vandenboom, R., Xeni, J., & Houston, M. E. (1998). Potentiation of in vitro concentric work in mouse fast muscle. *Journal of Applied Physiology*, *84*(1), 236-243.

Gregory, C. M., & Bickel, C. S. (2005). Recruitment patterns in human skeletal muscle during electrical stimulation. *Physical therapy*, *85*(4), 358-364.

Hamada, T., Sale, D. G., MacDougall, J. D., & Tarnopolsky, M. A. (2000). Postactivation potentiation, fiber type, and twitch contraction time in human knee extensor muscles. *Journal of applied physiology*, *88*(6), 2131-2137.

Hartshorne, D. J., Ito, M., & Erdödi, F. (2004). Role of protein phosphatase type 1 in contractile functions: myosin phosphatase. *Journal of Biological Chemistry*, *279*(36), 37211-37214.

Heckman, C. J., & Enoka, R. M. (2004). Physiology of the motor neuron and the motor unit. In *Handbook of Clinical Neurophysiology* (Vol. 4, pp. 119-147). Elsevier.

Heckman, C. J., & Enoka, R. M. (2012). Motor unit. *Comprehensive physiology*, *2*(4), 2629-2682.

Henneman, E. (1957). Relation between size of neurons and their susceptibility to discharge. *Science*, *126*(3287), 1345-1347.

Herzog, W., Powers, K., Johnston, K., & Duvall, M. (2015). A new paradigm for muscle contraction. *Frontiers in physiology*, *6*, 174.

Holobar, A., Farina, D., Gazzoni, M., Merletti, R., & Zazula, D. (2009). Estimating motor unit discharge patterns from high-density surface electromyogram. *Clinical Neurophysiology*, *120*(3), 551-562.

Hanson, J., & Huxley, H. E. (1957). Quantitative studies on the structure of cross-striated myofibrils: II. Investigations by biochemical techniques. *Biochimica et biophysica acta*, *23*, 250-260.

Huxley, H. E., & Hanson, J. (1957). Quantitative studies on the structure of cross-striated myofibrils: I. Investigations by interference microscopy. *Biochimica et biophysica acta*, *23*, 229-249.

Huxley, A. F., & Simmons, E. M. (1973, January). Mechanical transients and the origin of muscular force. In *Cold Spring Harbor Symposia on Quantitative Biology* (Vol. 37, pp. 669-680). Cold Spring Harbor Laboratory Press.

Inglis, J. G., Howard, J., McIntosh, K., Gabriel, D. A., & Vandenboom, R. (2011). Decreased motor unit discharge rate in the potentiated human tibialis anterior muscle. *Acta physiologica*, *201*(4), 483-492.

Kamm, K. E., & Stull, J. T. (2011). Signaling to myosin regulatory light chain in sarcomeres. *Journal of Biological Chemistry*, *286*(12), 9941-9947.

Klein, C. S., Ivanova, T. D., Rice, C. L., & Garland, S. J. (2001). Motor unit discharge rate following twitch potentiation in human triceps brachii muscle. *Neuroscience letters*, *316*(3), 153-156.

Klein, Rice, C. L., Ivanova, T. D., & Garland, S. J. (2002). Changes in motor unit discharge rate are not associated with the amount of twitch potentiation in old men. Journal of Applied Physiology, 93(5), 1616–1621. https://doi.org/10.1152/japplphysiol.00414.2002

Koubassova, N. A., & Tsaturyan, A. K. (2011). Molecular mechanism of actin-myosin motor in muscle. *Biochemistry (Moscow)*, *76*(13), 1484-1506.

Lännergren, J., Bruton, J. D., & Westerblad, H. (2000). Vacuole formation in fatigued skeletal muscle fibres from frog and mouse: effects of extracellular lactate. *The Journal of Physiology*, *526*(3), 597-611.

Lai, S., Collins, B. C., Colson, B. A., Kararigas, G., & Lowe, D. A. (2016). Estradiol modulates myosin regulatory light chain phosphorylation and contractility in skeletal muscle of female mice. *American Journal of Physiology-Endocrinology and Metabolism*, *310*(9), E724-E733.

Larsson, L., Edstrom, L., Lindegren, B., Gorza, L., & Schiaffino, S. (1991). MHC composition and enzyme-histochemical and physiological properties of a novel fast-twitch motor unit type. *American Journal of Physiology-Cell Physiology*, *261*(1), C93-C101.

Lehman, W., Rosol, M., Tobacman, L. S., & Craig, R. (2001). Troponin organization on relaxed and activated thin filaments revealed by electron microscopy and three-dimensional reconstruction. *Journal of molecular biology*, *307*(3), 739-744.

Levine, R. J., Kensler, R. W., Yang, Z., & Sweeney, H. L. (1995). Myosin regulatory light chain phosphorylation and the production of functionally significant changes in myosin head arrangement on striated muscle thick filaments. *Biophysical journal*, *68*(4 Suppl), 224S.

Levine, R. J., Kensler, R. W., Yang, Z., Stull, J. T., & Sweeney, H. L. (1996). Myosin light chain phosphorylation affects the structure of rabbit skeletal muscle thick filaments. *Biophysical journal*, *71*(2), 898-907.

Lewis, D. B., & Barclay, C. J. (2014). Efficiency and cross-bridge work output of skeletal muscle is decreased at low levels of activation. *Pflügers Archiv-European Journal of Physiology*, *466*(3), 599-609.

Linari, M., Brunello, E., Reconditi, M., Fusi, L., Caremani, M., Narayanan, T., ... & Irving, M. (2015). Force generation by skeletal muscle is controlled by mechanosensing in myosin filaments. *Nature*, *528*(7581), 276-279.

Lowey, S., & Trybus, K. M. (2010). Common structural motifs for the regulation of divergent class II myosins. *Journal of Biological Chemistry*, *285*(22), 16403-16407.

Macefield, V. G., Häger-Ross, C., & Johansson, R. S. (1996). Control of grip force during restraint of an object held between finger and thumb: responses of cutaneous afferents from the digits. *Experimental Brain Research*, *108*(1), 155-171.

MacIntosh, B. R., & Willis, J. C. (2000). Force-frequency relationship and potentiation in mammalian skeletal muscle. *Journal of Applied Physiology*, *88*(6), 2088-2096.

MacIntosh, B. R., Taub, E. C., Dormer, G. N., & Tomaras, E. K. (2008). Potentiation of isometric and isotonic contractions during high-frequency stimulation. *Pflügers Archiv-European Journal of Physiology*, *456*(2), 449.

MacIntosh, B. R. (2010). Cellular and whole muscle studies of activity dependent potentiation. *Muscle Biophysics*, 315-342.

Manning, D. R., & Stull, J. T. (1982). Myosin light chain phosphorylation-dephosphorylation in mammalian skeletal muscle. *American Journal of Physiology-Cell Physiology*, *242*(3), C234-C241.

McKillop, D. F., & Geeves, M. A. (1993). Regulation of the interaction between actin and myosin subfragment 1: evidence for three states of the thin filament. *Biophysical journal*, *65*(2), 693-701.

Milner-Brown, H. S., Stein, R. B., & Yemm, R. (1973). The orderly recruitment of human motor units during voluntary isometric contractions. *The Journal of physiology*, *230*(2), 359-370.

Moraczewska, J. (2002). Structural determinants of cooperativity in acto-myosin interactions. *Acta Biochimica Polonica*, *49*(4), 805-812.

Morgan, Margaret, Perry, S. V., & Ottaway, J. U. N. E. (1976). Myosin light-chain phosphatase. *Biochemical Journal*, *157*(3), 687-697

Morris, S. R., Gittings, W., & Vandenboom, R. (2018). Epinephrine augments posttetanic potentiation in mouse skeletal muscle with and without myosin phosphorylation. *Physiological Reports*, *6*(9), e13690.

Nielsen, B. G. (2009). Calcium and the role of motoneuronal doublets in skeletal muscle control. *European Biophysics Journal*, *38*(2), 159.

Padre, R. C., & Stull, J. T. (2000). Conformational requirements for Ca2+/calmodulin binding and activation of myosin light chain kinase. *FEBS letters*, *472*(1), 148-152.

Patel, J. R., Diffee, G. M., Huang, X. P., & Moss, R. L. (1998). Phosphorylation of myosin regulatory light chain eliminates force-dependent changes in relaxation rates in skeletal muscle. *Biophysical journal*, *74*(1), 360-368.

Perrier, J. F., & Cotel, F. (2015). Serotonergic modulation of spinal motor control. *Current opinion in neurobiology*, *33*, 1-7.

Perry, S. V. (1998). Troponin T: genetics, properties and function. *Journal of Muscle Research & Cell Motility*, *19*(6), 575-602.

Phillips Jr, G. N., Fillers, J. P., & Cohen, C. (1986). Tropomyosin crystal structure and muscle regulation. *Journal of molecular biology*, *192*(1), 111-127.

Piazzesi, G., Caremani, M., Linari, M., Reconditi, M., & Lombardi, V. (2018). Thick filament mechano-sensing in skeletal and cardiac muscles: a common mechanism able to adapt the energetic cost of the contraction to the task. *Frontiers in physiology*, *9*, 736.

Powers, K., Schappacher-Tilp, G., Jinha, A., Leonard, T., Nishikawa, K., & Herzog, W. (2014). Titin force is enhanced in actively stretched skeletal muscle. *Journal of Experimental Biology*, *217*(20), 3629-3636.

Rassier, D. E., & MacIntosh, B. R. (2002). Sarcomere length-dependence of activity-dependent twitch potentiation in mouse skeletal muscle. *BMC physiology*, *2*(1), 1-8.

Rayment, I. (1996). The structural basis of the myosin ATPase activity. *Journal of Biological Chemistry*, *271*(27), 15850-15853.

Rayment, I., Holden, H. M., Whittaker, M., Yohn, C. B., Lorenz, M., Holmes, K. C., & Milligan, R. A. (1993). Structure of the actin-myosin complex and its implications for muscle contraction. *Science*, *261*(5117), 58-65.

Reconditi, M., Linari, M., Lucii, L., Stewart, A., Sun, Y. B., Boesecke, P., ... & Irving, M. (2004). The myosin motor in muscle generates a smaller and slower working stroke at higher load. *Nature*, *428*(6982), 578-581.

Reggiani, C., Bottinelli, R., & Stienen, G. J. (2000). Sarcomeric myosin isoforms: fine tuning of a molecular motor. *Physiology*, *15*(1), 26-33.

Sargeant, A. J. (2007). Structural and functional determinants of human muscle power. *Experimental physiology*, *92*(2), 323-331.

Schiaffino, S., & Reggiani, C. (2011). Fiber types in mammalian skeletal muscles. *Physiological reviews*, *91*(4), 1447-1531.

Sheetz, M. P., & Spudich, J. A. (1983). Movement of myosin-coated fluorescent beads on actin cables in vitro. *Nature*, *303*(5912), 31-35.

da Silva, A. C. R., & Reinach, F. C. (1991). Calcium binding induces conformational changes in muscle regulatory proteins. *Trends in biochemical sciences*, *16*, 53-57.

Smith, N. P., Barclay, C. J., & Loiselle, D. S. (2005). The efficiency of muscle contraction. *Progress in biophysics and molecular biology*, *88*(1), 1-58.

Smith, I. C., Gittings, W., Huang, J., McMillan, E. M., Quadrilatero, J., Tupling, A. R., & Vandenboom, R. (2013). Potentiation in mouse lumbrical muscle without myosin light chain phosphorylation: is resting calcium responsible?. *Journal of General Physiology*, *141*(3), 297-308.

Smith, D. A. (2018). *The Sliding-Filament Theory of Muscle Contraction*. Springer International Publishing.

Stewart, M., & Kensler, R. W. (1986). Arrangement of myosin heads in relaxed thick filaments from frog skeletal muscle. *Journal of molecular biology*, *192*(4), 831-851.

Stewart, M. A., Franks-Skiba, K., Chen, S., & Cooke, R. (2010). Myosin ATP turnover rate is a mechanism involved in thermogenesis in resting skeletal muscle fibers. *Proceedings of the National Academy of Sciences*, *107*(1), 430-435.

Stull, J. T., Kamm, K. E., & Vandenboom, R. (2011). Myosin light chain kinase and the role of myosin light chain phosphorylation in skeletal muscle. *Archives of biochemistry and biophysics*, *510*(2), 120-128.

Sweeney, H. L., Bowman, B. F., & Stull, J. T. (1993). Myosin light chain phosphorylation in vertebrate striated muscle: regulation and function. *American Journal of Physiology-Cell Physiology*, *264*(5), C1085-C1095.

Tomalka, A., Weidner, S., Hahn, D., Seiberl, W., & Siebert, T. (2020). Cross-bridges and sarcomeric non-cross-bridge structures contribute to increased work in stretch-shortening cycles. *Frontiers in physiology*, *11*, 921.

Vandenboom, R., Grange, R. W., & Houston, M. E. (1993). Threshold for force potentiation associated with skeletal myosin phosphorylation. *American Journal of Physiology-Cell Physiology*, *265*(6), C1456-C1462.

Vandenboom, R., Hannon, J. D., & Sieck, G. C. (2002). Isotonic force modulates force redevelopment rate of intact frog muscle fibres: evidence for cross-bridge induced thin filament activation. *The Journal of physiology*, *543*(2), 555-566.

Vandenboom, R., Gittings, W., Smith, I. C., Grange, R. W., & Stull, J. T. (2013). Myosin phosphorylation and force potentiation in skeletal muscle: evidence from animal models. *Journal of muscle research and cell motility*, *34*(5), 317-332.

Vandenboom, R. (2016). Modulation of skeletal muscle contraction by myosin phosphorylation. Compr Physiol 7: 171–212.

Wakabayashi, K., Sugimoto, Y., Tanaka, H., Ueno, Y., Takezawa, Y., & Amemiya, Y. (1994). X-ray diffraction evidence for the extensibility of actin and myosin filaments during muscle contraction. *Biophysical journal*, *67*(6), 2422-2435.

Westerblad, H., Duty, S., & Allen, D. G. (1993). Intracellular calcium concentration during low-frequency fatigue in isolated single fibers of mouse skeletal muscle. *Journal of Applied Physiology*, *75*(1), 382-388.

Woodhead, J. L., Zhao, F. Q., Craig, R., Egelman, E. H., Alamo, L., & Padrón, R. (2005). Atomic model of a myosin filament in the relaxed state. *Nature*, *436*(7054), 1195-1199.

Woods, J. J., Furbush, F., & Bigland-Ritchie, B. (1987). Evidence for a fatigue-induced reflex inhibition of motoneuron firing rates. *Journal of neurophysiology*, *58*(1), 125-137.

Wray, J. S., Vibert, P. J., & Cohen, C. (1975). Diversity of cross-bridge configurations in invertebrate muscles. *Nature*, *257*(5527), 561-564.

Xeni, J., Gittings, W. B., Caterini, D., Huang, J., Houston, M. E., Grange, R. W., & Vandenboom, R. (2011). Myosin light-chain phosphorylation and potentiation of dynamic function in mouse fast muscle. *Pflügers Archiv-European Journal of Physiology*, *462*(2), 349-358.

Xu, S., Offer, G., Gu, J., White, H. D., & Yu, L. C. (2003). Temperature and ligand dependence of conformation and helical order in myosin filaments. *Biochemistry*, *42*(2), 390-401.

Zhi, G., Ryder, J. W., Huang, J., Ding, P., Chen, Y., Zhao, Y., ... & Stull, J. T. (2005). Myosin light chain kinase and myosin phosphorylation effect frequency-dependent potentiation of skeletal muscle contraction. *Proceedings of the National Academy of Sciences*, *102*(48), 17519-17524.